

The FUSE Observer's Guide

Version 8.0, August 3, 2006.

Edited by
B-G Andersson

Including contributions from:
Ravi Sankrit, Jean Dupuis, Bill Blair, Bill Oegerle,
Jeff Kruk, Scott Friedman, Tom Ake, Ed Murphy,
Alex Fullerton, Jerry Kriss, Dave Sahnou, Hal Weaver and Rich
Robinson

Major version 8.0 changes from version 7.0:

- For Cycle 8 targets must be above absolute declinations above 50 degrees, except for certain lower declination targets (Sec. 1.2.1).
- Because of alignment difficulties, LWRS is again the default aperture for all observations (TTAG and HIST mode) (Sec 3.1)
- For SiC ONLY and LiF2-HIRS ONLY observations, the bright limit is now 5.0×10^{-10} ergs $\text{cm}^{-2} \text{s}^{-1} \text{\AA}^{-1}$.

Table of Contents

[1. Introduction and Overview](#)

- [1.1 The FUSE Mission](#)
- [1.2 Mission Operations](#)
- [1.2.1 Scheduling Constraints](#)

[2. Instrument Overview](#)

- [2.1 Optical Design](#)
- [2.2 Telescope Mirrors](#)
- [2.3 Focal Plane Assemblies](#)
- [2.4 Spectrograph](#)
 - [2.4.1 Wavelength Coverage and Dispersion](#)
 - [2.4.2 Effective Area](#)
 - [2.4.3 Spectroscopic Resolving Power](#)
 - [2.4.4 Spectral Astigmatism](#)
- [2.5 Detectors](#)
 - [2.5.1 Detector Background](#)
 - [2.5.2 Detector Flat Field](#)
 - [2.5.3 Detector X-Walk](#)
 - [2.5.4 Worms](#)
- [2.6 Fine Error Sensor Cameras](#)
- [2.7 Instrument Data System](#)

[3. Planning Observations](#)

- [3.1 Brief Guide for Proposers](#)
 - [3.1.1 Choosing Apertures](#)
 - [3.1.2 Flux Range](#)
 - [3.1.3 Observing Modes and Observation Types](#)
 - [3.1.4 Signal to Noise and Exposure Time Calculations](#)
 - [3.1.5 Target Acquisition](#)
 - [3.1.6 Scheduling Considerations](#)
- [3.2 Observing modes](#)
 - [3.2.1 Time Tag \(TTAG\)](#)
 - [3.2.2 Spectral Image or Histogram \(HIST\)](#)
 - [3.2.3 Snapshots](#)
 - [3.2.4 Focal Plane Splits](#)
 - [3.2.5 FES Images](#)
 - [3.2.6 Unsupported Modes](#)
- [3.3 Estimating Exposure Times](#)
- [3.4 Scheduling](#)
- [3.5 Target Acquisition](#)
 - [3.5.1 General Field Acquisition](#)
 - [3.5.2 Types of Target Acquisition](#)
 - [3.5.3 Target Centering in Aperture](#)
 - [3.5.4 Optically Very Bright Targets](#)
 - [3.5.6 Extended Targets](#)
 - [3.5.6 Targets in Crowded Fields](#)
 - [3.5.7 Moving Targets](#)
- [3.6 Restrictions](#)
 - [3.6.1 Short Observations and Minimum Observing Time](#)
 - [3.6.2 Bright Targets](#)
 - [3.6.3 Night Only Observations](#)
 - [3.6.4 Signal to Noise Ratio Limits](#)
 - [3.6.5 Moving Target Restrictions](#)
 - [3.6.6 Slit Position Angle Constraints](#)
 - [3.6.7 Beta Angle Constraints](#)
 - [3.6.8 Ram Angle Avoidance Constraints](#)
 - [3.6.9 Magnetic Torque Authority](#)
- [3.7 Time Critical and Monitoring Observations](#)

[4. Science Data Processing](#)

- [4.1 The FUSE Pipeline Processing System](#)
 - [4.1.1 Processing FUV Spectral Data](#)
 - [4.1.2 Processing FES CCD Images](#)
- [4.2 Data Distribution](#)
- [4.3 Data Analysis Tools](#)

[5. Further References](#)

Appendices

Note: These appendices were taken from earlier versions of the FUSE Observer's Guide, and contain some dated material. However, they do contain more detailed discussion of some items and issues, and are linked here for reference. In any cases of overlapping information, the material in the main document takes precedence.

[Appendix A: Signal-to-noise Calculations and Examples](#)

[Appendix B: Acquisition Types Discussion](#)

1. Introduction and Overview

The FUSE Observer's Guide is intended as the primary source of information regarding the FUSE satellite, instrument and data for current and prospective users of the instrument. While this document should provide the necessary background and information for most users additional information, on specific topics, is available in the following documents:

- The FUSE Data Handbook - describes the FUSE data, including instrumental effects
- The CalFUSE Pipeline Reference Guide - details the CalFUSE data reduction pipeline
- The FUSE Data Analysis Cookbook - for an introduction to manipulating post-pipeline FUSE data

Additional documentation, FUSE specific software, and interactive tools observation planning, can be found on the FUSE/JHU web site at:

<http://fuse.pha.jhu.edu>

For proposal specific issues, further information can be found at the NASA Guest Investigator web site:

<http://fusegi.pha.jhu.edu>

Documents at this site include the NASA Research Announcement (NRA) for the current cycle, Phase 1 and 2 proposal instructions, template files as well as lists of previously observed and pending targets. For further details, technical questions or general help, please contact FUSE User Support at: fuse_support@pha.jhu.edu.

Version 8.0 of the FUSE Observer's Guide was updated in the summer of 2006 in preparation for the cycle 8 and contains the most up-to-date information available at the time of writing. However, as several operational issues and procedures are still in a state of flux, please consult the FUSE web site for updates and additional information.

Sections 1.1 & 1.2 of the *Guide* are intended to provide an overview of the mission and its practical implementation. This is followed by an overview of the FUSE instrument in section 2. Section 3 provides additional information to assist in designing and preparing for FUSE observations. Detailed discussions of selected topics can be found in the appendices to this *Guide*.

1.1 The FUSE Mission

The Far Ultraviolet Spectroscopic Explorer (FUSE) mission provides access to the 905-1187 Å spectral region with a resolving power of ~20,000 and is the only currently active mission to provide access to this spectral range. In the 1970s, the *Copernicus* mission opened the far-ultraviolet (FUV) universe by obtaining spectra of bright, hot stars within ~1 kpc of the Sun. Two telescopes, the *Hopkins Ultraviolet Telescope* (HUT) and the *Orbiting Retrievable Far and Extreme Ultraviolet Spectrometers* (ORFEUS), flown on Space Shuttle missions in the 1990s, have also provided brief glimpses at lower spectral resolution into the FUSE wavelength range. FUSE is able to observe sources more than 10,000 times fainter than *Copernicus* at a resolution many times better than that obtainable with either HUT or ORFEUS. This increase in sensitivity enables FUSE to explore the outer reaches of the Milky Way and also makes it possible to use quasars and active galactic nuclei as continuum sources for absorption line studies of distant gas clouds.

FUSE is a "Principal Investigator-class" mission, and as such was developed to carry out several primary scientific objectives proposed by the PI science team and selected by NASA. The satellite was launched on June 24, 1999 into a 768 km (101 min.) circular orbit, with a 25 degree inclination to the equator. In the prime mission (cycles 1-3) about half of the available observing time was allocated to the PI team to accomplish the goals associated with these objectives. The main goals included:

- Determining the abundance of deuterium in a wide range of Galactic environments having different metallicities and evolutionary histories.
- Conducting a survey of OVI absorption in the Milky Way disk and halo and the Magellanic clouds, in order to determine the physical properties and distribution of hot gas.
- Exploring the nature and distribution of the hot intergalactic medium (IGM).

Several medium and small PI team projects were also undertaken addressing a range of topics such as: AGNs, H₂ and different kinds of stars. Listings of, and abstracts for, these programs can be found on the FUSEGI website (<http://fusegi.pha.jhu.edu>)

Many results from these programs have already been published in the literature. A survey of the ADS database will provide the current status of FUSE based research. In particular we draw your attention to the three special issues of the *Astrophysical Journal*; ApJL vol. 538, No. 1, Part 2, containing results from the Early Release Observations, ApJS vol 140, no. 1., containing the initial results from the FUSE study of the D/H ratio and ApJS vol. 146, No. 1. containing results from FUSE surveys of OVI in the Galactic halo and high-velocity clouds.

Cycle 8 marks the fifth year of the FUSE extended mission. As in cycles 4-7, all of the available observing time will be allocated through the NRA process to Guest Investigator programs. Details of the satellite capabilities and rules and constraints for the proposal cycle can be found below in this document and in documents posted on the FUSEGI website (<http://fusegi.pha.jhu.edu>).

1.2 Mission Operations

Science and mission operations are conducted from the FUSE Science Center on the Homewood Campus of the Johns Hopkins University (JHU). Functions include planning and scheduling of observations, generation of command loads, communication with the satellite through an autonomous ground station, receipt and processing of science and engineering data, monitoring of the health and safety of the satellite and instrument, computation of the FUSE orbital elements, off-line analyses of science and engineering data, and maintenance of flight software.

In this section we provide an overview of the procedures and main constraints of the planning and scheduling process. This is intended to provide the prospective user enough background to understand when and why FUSE observations can and cannot be made and under what circumstances special justification of observational procedures may be needed. Further detail can be found in section 3 this document and on the FUSE web site.

Based on the target database, scientific and spacecraft constraints, FUSE Mission Planning (MP) generates Long Range Plans (LRP) and Mission Planning Schedules (MPS). The LRP covers a year's worth of observations and permits tracking of time critical observations and facilitates producing efficient timelines. However, many of the details in producing optimum observing sequences cannot be fully coded into the LRP. Hence, the actual target selections are done at the time of the MPS generation. Observations in the LRP which are not included into a given MPS are returned to the target pool and the LRP is regenerated. The LRP is on average regenerated once a week. Therefore, the FUSE LRP is a highly dynamical document (not comparable to the HST version) and thus, while invaluable to the FUSE project, is of very limited direct use to the user community. The Mission Planning Schedules (MPS) typically covers a few days to a week's worth of observations and is the input for the command loads sent to the spacecraft. The MPS is generated to achieve a maximum efficiency of science observations, while taking spacecraft and scientific constraints into account. The main spacecraft constraints are:

- Availability of magnetic torque authority (see sec. 3.6.9)
- Reaction wheel momentum management (see sec 3.6.10)
- Allowed range of beta (anti-Sun) angle and minimization of short term variation in beta angle (see sec. 3.6.7)

- Avoidance of the orbital RAM zone (see sec. 3.6.8)

Each of these will be briefly discussed below. Because of the dynamical nature of the reaction wheel momentum management, a reliable prediction of target availability as a function of time is difficult. While the current attitude control system is being optimized, tools to accomplish this are also under development. For this reason only very limited time-constraints are allowed in cycle 8 programs. Users may consult the FUSE Slit Position Angle/Beta Angle Calculator, available at the FUSE web site to estimate the rough availability of a target over the course of the year.

With the transition to **extended mission operations** several additional *de facto* constraints come into play. The FUSE operations staff is shrinking, and in particular, in the Spacecraft Control Center which is transitioning from a 24/7 schedule to a 16 hour M-F (no holiday) schedule. This has the potential of significantly impacting such things as anomaly recovery and target-of-opportunity response times. Also on the Science Operations side, similar restrictions come into play. While we strive to minimize the impact on the FUSE user, some impacts are unavoidable.

1.2.1 Scheduling Constraints

The instant and time-averaged scheduling availability of a given target depends on several factors. Two constraints originated already in the mission design and additional considerations have arisen due to spacecraft anomalies. In order to maintain the required power-positive configuration of the spacecraft and its solar panels with respect to the Sun, as well as safeguarding the detectors from direct sunlight, FUSE must point only within a limited range of anti-sun angles ("beta angle"; sec 3.6.7). In addition, as the optics materials are prone to degradation if exposed to the residual terrestrial atmosphere at the FUSE orbit altitude (primarily atomic oxygen), the FUSE project has been careful to minimize this degradation by keeping the spacecraft from pointing in the direction of the orbital plane ("RAM avoidance"; sec. 3.6.8). This strategy has proven highly successful yielding a much slower sensitivity degradation over time than earlier FUV missions. With the shrinkage of the Earth's atmosphere, following the lowered Solar activity as we enter the Solar cycle minimum, the RAM avoidance constraint has now been dropped.

The attitude control of the spacecraft is accomplished through a combination of reaction wheels and magnetic torquer bars (MTB). In the original spacecraft configuration the attitude control was fully accomplished by the four on-board reaction wheels, with the MTBs serving to keep the reaction wheels from spinning up to unacceptably large rotation speeds. After the loss of the first two reaction wheels in December 2001, a hybrid attitude control scheme was designed with the MTBs serving both their original purpose as well as being used directly for attitude control, but with the remaining two reaction wheels still the primary control mechanism. Following the loss of the third reaction wheel in December 2004, a further modification of the attitude control scheme has now been implemented. However, with this latest anomaly, the planning constraints on the observatory have changed significantly.

While the restrictions in beta angle are still in effect, the main planning constraints for the current spacecraft configuration consist of the requirement for instantaneous torque-authority (i.e. the need for sufficient control torque to counter-balance the external disturbances on the spacecraft) and the requirement to keep the remaining reaction wheel from spinning up to saturation speeds. These two requirements limit both the short-time sky availability and the duration and cadence of allowable pointings.

The primary area of instantaneous torque-authority consists of an irregularly shaped and quite dynamic region in the vicinity of the FUSE orbital poles (at declination ± 65 deg.). Over the 60 day precession cycle these regions combine to cover the equatorial polar caps down to about $|\text{Dec.}|=50$ degrees. Combined over a year, this recurring pattern can allow substantial amounts of potential observing time for targets at high declination. Localized areas of torque authority exist also at low declinations. The FUSE project expects to be able to access these in a limited fashion during Cycle 8.

The requirement to manage the rotation speed on the remaining reaction wheel imposes further planning and scheduling constraints, which limit the length and absolute timing of individual observations. Therefore, ephemerid specific observations will not be considered in cycle 8 and while substantial total exposure times can be achieved, long observations will likely consist of multiple, moderate length, individual integrations.

2. The Instrument

2.1 Optical Design

The FUSE instrument (Figure 2.1-1) is based on a Rowland circle design and consists of four separate optical paths or channels. A channel consists of a mirror, a Focal Plane Assembly (FPA, which includes the spectrograph apertures), a diffraction grating, and a portion of an FUV detector. The channels are co-aligned so that light from a single target properly enters the apertures on all four channels, thereby maximizing the throughput of the instrument. This is accomplished with actuators on the mirror assemblies and the FPAs. As noted above in section 1.2, the alignment of these channels has become a major driver in the way FUSE observations are accomplished.

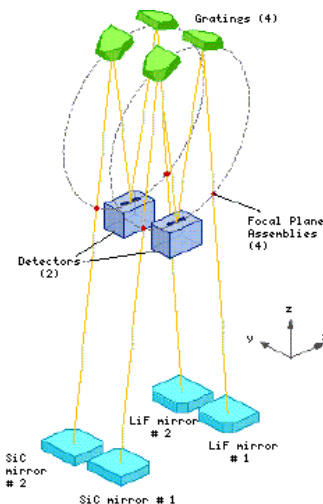


Figure 2.1-1. Optical layout of FUSE instrument showing the four-channel design.

This multi-channel design allowed the coatings on the mirrors and gratings to be selected to maximize reflectivity in the wavelength ranges above and below ~ 1020 Å. Two mirrors and two gratings are coated with Silicon Carbide (SiC) to provide wavelength coverage below 1020 Å, while the other two mirrors and gratings are coated with aluminum and a Lithium Fluoride (LiF) overcoat. The Al+LiF coating provides about twice the reflectivity of SiC at wavelengths > 1050 Å, but has very little reflectivity below 1020 Å. We will thus refer to "the SiC channels" and the "LiF channels" below.

The four channels can be thought of as comprising two nearly identical "sides" of the instrument. A side consists of one LiF and one SiC channel, each of which produces a spectrum that falls onto a single detector. Each channel has a bandpass of about 200 Å. Thus, at least two channels, one LiF and one SiC, are required to cover the entire ~ 290 Å wavelength range of the instrument. All four channels cover the 1015-1075 Å region.

Figure 2.1-1 also shows the orientation of the instrument prime coordinate system (X,Y,Z). The two LiF channels are on the +X side of the instrument, which is nominally kept in the shade (i.e., the -X side always points toward the sun). This orientation minimizes the amount of sunlight that can make its way down the baffles surrounding the LiF channels. Minimizing stray light in the LiF channels is crucial to the operation of the Fine Error Sensor (FES) guidance camera which operates at visible wavelengths. The orientation of the satellite is actually biased by 2.5° (in roll around the Z axis) in order to keep the radiator of the operational FES in the shade.

During initial checkout, it was determined that FES-A performed better and it was hence designated the prime FES. This was true for all observations up until December 2004. Due to intermittent problems with FES-A, initially encountered in the spring of 2005, the FUSE project switched to FES-B as the default Guide Camera in July 2005. As FES-B views the

Focal Plane Assembly (FPA) in the LiF2 channel, the most reliable (and well centered) data will now occur in LiF2(A & B), rather than in LiF1.

After the FUV focus in LiF2 was optimized early in the mission, the image quality in FES-B was marginal for guiding purposes. In order to improve the image quality in FES-B, the LiF2 FPA has been moved to a position that is offset from the focal plane of the LiF2 primary mirror. The spectral resolution in LiF2 is unaffected for observations of point sources, but the throughput of the narrow apertures will be reduced. The effective transmission of the apertures has not yet been characterized in detail, but it is expected to be approximately 70% for MDRS and 15% for HIRS. These factors have been incorporated into the on-line Exposure Time Calculator (ETC). The resolution for observations of diffuse sources in LiF2 is expected to degrade slightly.

2.2 Telescope Mirrors

The four telescope mirrors are identical off-axis paraboloids except that the off-axis angle of the SiC mirrors and the LiF mirrors differ slightly. This angle is defined by aperture stops placed over the surfaces of the mirrors. The mirror coatings also vary, with two mirrors being coated with silicon carbide, SiC, and two being coated with aluminum with a protective overcoat of lithium fluoride (LiF). Three stepper-motor actuators are attached to the rear of each mirror, which allow tip-tilt-focus adjustments. The tip-tilt mechanism is used to provide rough alignment of the mirrors to the Focal Plane Assembly entrance apertures (see next section). The point spread function (PSF) at the focal plane places 90% of the light within a diameter of 1.5 arcsec. More details are provided in Appendix A, and some of the specifications of the mirror assemblies are given in Table A.2-1.

2.3 Focal Plane Assemblies

At the focus of each telescope mirror is a Focal Plane Assembly (FPA) that acts as the optical entrance aperture for each spectrograph channel. An FPA consists of an optical flat mirror mounted on a two-axis flight-adjustable stage. As summarized in Table 2.3-1, four apertures are cut into the flat. The apertures are not shuttered, and always allow light (even if it is only from the sky) to fall on the grating, which is then dispersed onto the detector.

The front surface of the FPAs on the two LiF channels are reflective in visible light. Light not passing through the apertures is reflected into one of two visible light CCD cameras (FES). Only one camera is in use at a given time and guiding is slaved to this channel. Images of stars in the field of view (FOV) around the apertures are used for acquisition and guiding by the camera system. Further information on the FES cameras is contained in [Section 2.6](#).

In the summer of 2004 the default aperture for bright target observations (HIST) was changed to MDRS in order to conserve the sensitivity of the detectors in the areas corresponding to LWRS. However, with the increased difficulties associated with channel alignment in the one reaction wheel attitude control mode, LWRS is as of the Cycle 8 proposal round again the default aperture for all observations. For HIST mode observations where high precision data is required close to one of the brighter terrestrial air-glow lines, MDRS should be used. (see section 2.5.3)

The four apertures are:

- A large square aperture (LWRS: 30×30 arcsec; DEFAULT APERTURE), which can be used for observations of faint extended objects, producing a filled-aperture resolution of about ($\sim 100 \text{ km s}^{-1}$), or for point source observing. In principle, in the limit where telescope PSF and pointing stability are at the specs, this aperture provides a spectral resolution for point sources comparable to that obtained in the HIRS and MDRS apertures, except for any airglow lines. In practice, differential thermally-induced image motions produce a smearing effect that compromises spectral resolution somewhat. For TTAG mode observations, the thermal motions can be modeled and removed, to first order, gaining most resolution back. However, this procedure does not work for HIST mode observations, and is only partially successful for the SiC channels where the thermal motions are less well-behaved.
- The medium resolution aperture (MDRS: 4.0×20 arcsec) provides high throughput while minimizing airglow contamination. However, thermal drifts of the separate channels, and in particular of the SiC channels with respect to the LiF2 channel. For observations of bright targets, place in MDRS due to the above rule, the exposure time requested in a proposal should be doubled compared to the nominal results of the FUSE Exposure Time Calculator, in order to account for alignment shift. This does not apply to observations for which only LiF2 data are required. Note, however, that with the switch to FES-B, the throughput for MDRS and HIRS in LiF2 have degraded (see section 2.1, above).
- The high resolution aperture (HIRS: 1.25×20 arcsec), to ensure that maximum resolution is maintainable even if the telescope imaging or pointing stability degrade below specifications. (This is not a problem to date.) This aperture does not allow all of the light from a point source into the spectrograph, however, and maintaining alignment of four channels with these apertures is not practical currently due to thermally-induced mirror motions (see section 1.2.1). Observations using only the LiF2 channel are possible with this aperture size, however.
- A pinhole aperture (PINH: approximately 0.5 arcsec in diameter) The pinhole was designed for possible use in observations of very bright targets, for which FUSE has not been optimized. *Using extensive data sets from co-added exposures of airglow emission we have performed a search for signals from the pinhole apertures. Based on the known relative areas of the four apertures and the lack of any detected signal associated with the pinhole apertures, we have concluded that the pinholes must have become blocked. The use of this aperture is therefore not possible.*

Table 2.3-1: Apertures

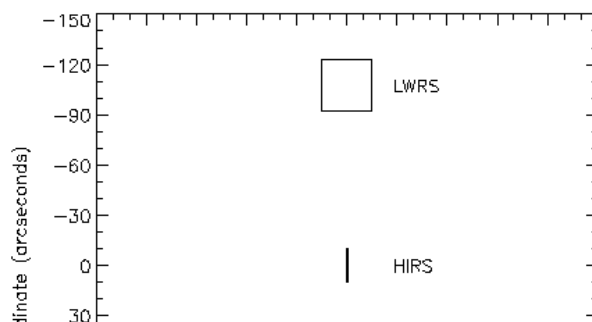
Aperture	Keyword	Dimensions (arcsec)	Throughput (approximate)	Throughput LiF2 (approximate)
large square	LWRS	30×30	1.00	1.0
medium rectangle	MDRS	4.0×20	0.98	0.7
narrow rectangle	HIRS	1.25×20	0.85	0.15
pinhole Not Available	PINH	~ 0.5 (diameter)	~ 0.10	

Notes to Table 2.3-1: The aperture throughputs are computed assuming nominal PSF (90% encircled energy in 1.5 arcsec diameter), no pointing jitter, and source centered in the aperture. The lower throughput in LiF2 is only valid for observations performed with FES-B being used for acquisition and guiding. FES-B was made the default guide camera in July 2005. However, *effective* throughputs in MDRS and HIRS apertures can be considerably lower due to thermally-induced image motions, which vary on an individual pointing basis.

The pinhole aperture is not in use and is shown only for completeness.

The lower throughput in LiF2 is only valid for observations performed with FES-B being used for acquisition and guiding.

The geometrical arrangement of the apertures, drawn to scale, is shown below in Figure 2.3-1.



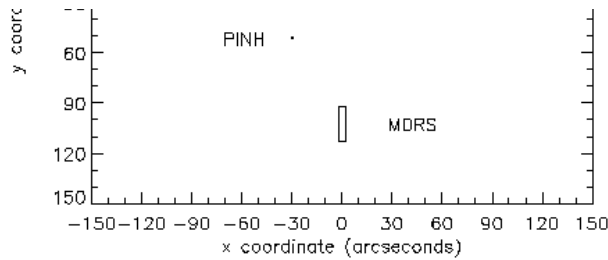


Figure 2.3-1. The locations of the FUSE apertures on the sky for an aperture position angle of 0° with North in the -Y direction. Positive aperture position angles correspond to a counter-clockwise rotation of the apertures on the sky. The so-called "reference point," used in some acquisition modes, is located at (X,Y) = (+60,0), or approximately an arcminute to the right of the HIRS aperture center. In these coordinates, the center of the slits are located at Y=-90.18 (MDRS), Y=10.27 (HIRS) and Y=118.07 (LWRS). (This figure does NOT represent the entire field of view of the FES camera.)

Each FPA can be moved independently in two directions. Motion tangential to the Rowland circle, which is roughly in the dispersion direction and perpendicular to the apertures, allows co-alignment of the channels and permits "focal plane splits" for high signal/noise ratio observations of bright targets. Motion in "Z" (perpendicular to the plane of the FPA mirror) enables focusing of the apertures with respect to the mirrors and the detector. The FPAs have no Y adjustment. Any Y corrections to alignment must be corrected by moving the appropriate mirror.

2.4 Spectrograph

The spectrograph has a Rowland circle design, with a diameter of 1652 mm. Light entering the spectrograph through an FPA aperture illuminates one of four diffraction gratings. The gratings are holographically ruled on spherical substrates made of fused silica. See Table A.4-1 for some of the design parameters of the spectrograph and diffraction gratings.

2.4.1 Wavelength Coverage and Dispersion

FUSE obtains spectra from about 905 Å to 1187 Å. The spectra from the four channels are imaged onto two microchannel plate detectors. Each detector has one SiC spectrum and one LiF spectrum imaged onto it, and therefore covers the entire wavelength range. The two channels are offset on the detector perpendicular to the dispersion direction to prevent the spectra from overlapping, and the dispersion direction is opposite for SiC and LiF spectra. (See Figure 2.4.1-1.) Each detector is divided into two functionally independent segments (A and B) separated by a small gap. To ensure that the gaps do not fall at the same wavelength region in both detectors, they are offset slightly with respect to each other. Table 2.4.1-1 lists the wavelength coverage of each of the eight detector segment/channel combinations. Nearly the entire wavelength range is covered by more than one channel, and the important 1015-1075 Å range is covered by all four, providing the highest effective area and the greatest redundancy.

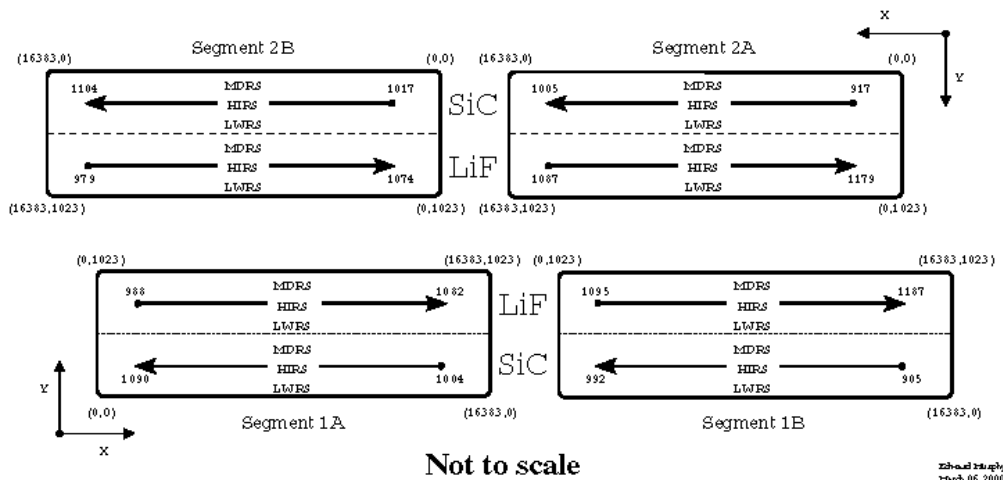
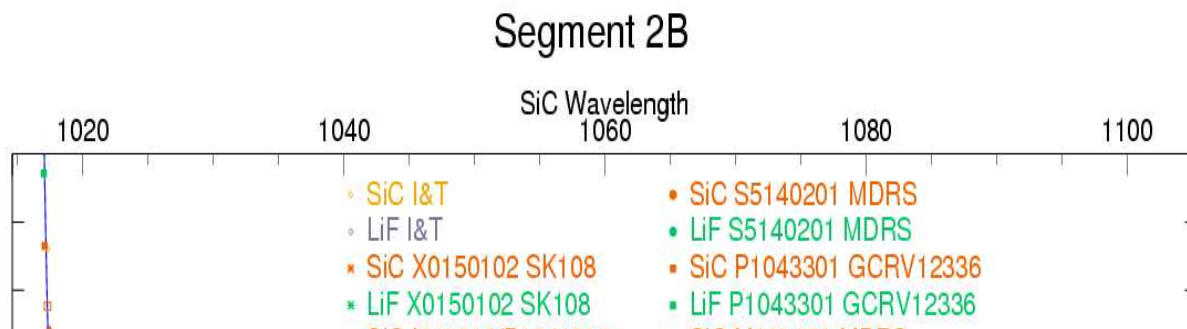


Figure 2.4.1-1 Wavelength coverage, dispersion directions, and image locations for the FUSE detectors. In this figure, the coordinate system as used for the detectors is shown, where X is the dispersion axis.

The SiC channels have a dispersive plate scale of 1.03 Å/mm while the LiF channels have a scale of 1.12 Å/mm. Coupled with the size of the detector pixels, this results in a scale of ~6.7 mÅ/pixel in the LiF channel and ~6.2 mÅ/pixel in the SiC channel (in the X or dispersion direction). (Note: one spectrograph resolution element is 6 - 10 detector pixels.)

As FUSE does not carry a wavelength calibration lamp, we have used a number of astronomical sources to establish the dispersion solution of the spectrograph. We use primarily the lines of molecular hydrogen in combination with low ionization atomic lines (particularly at wavelengths longward of 1108 Å). The relative dispersion solution has a scatter of about 5 pixels, except for a few regions where localized distortions of up to twice this value exist. At the edges of each detector the dispersion solution also deteriorates. However, the wavelength scale for a given observation has a variable 0-point offset, due to the location of the target within the slit, as well as effects caused by the grating motion. Work is under way to characterize these offsets and correct the effects due to them, to the extent possible, in the absolute wavelength scale in FUSE data. In figure 2.4.1-1 we show a plot of the residuals in the dispersion solution for detector segment 2B. Similar plots for all the detector segments can be found in the on-line "white paper" on the FUSE wavelength calibration (http://fuse.pha.jhu.edu/analysis/califuse_wp1.html), which also contains further discussion and details of the wavelength calibration. Note that recent results, based on astronomical observations (Bowen et al., 2006, in preparation) shows that observations of the same target taken at different times have an internal dispersion in the 0-point less than the FUSE resolution element (on LiF1; c.f. the [wavelength white paper](#))



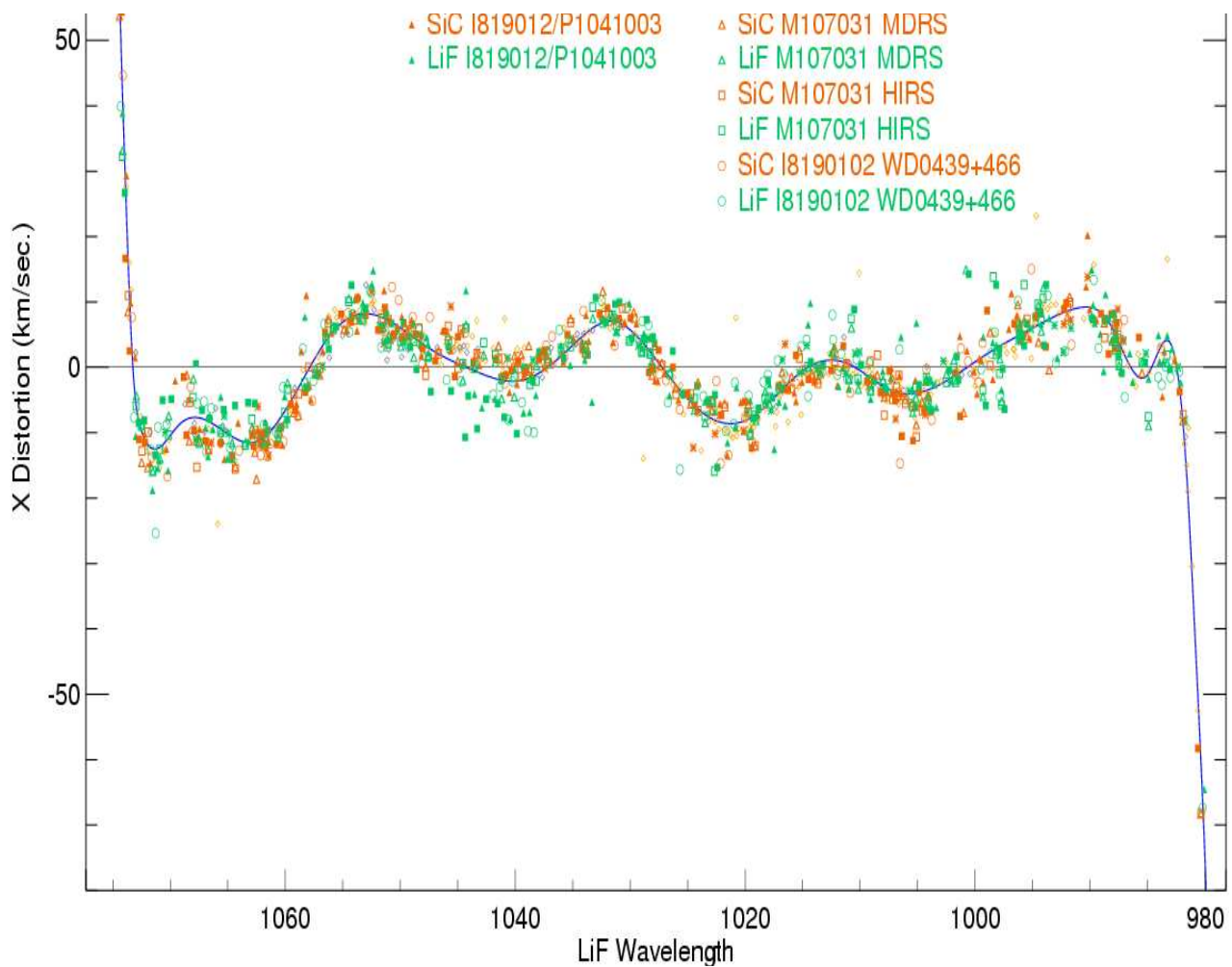


Figure 2.4.2-1 The in-flight derived dispersions solution - here for detector 2B. The (non-linear part of the) measured positions of interstellar absorption lines for a large number of sources, through the three main apertures, are plotted with a best fit. The residual around the fit is about 5 pixels or 2/3 of a resolution element (see section 2.4.3 below). Larger, localized, high frequency distortions do exist. Also, near the edges of each detector the wavelength solution deteriorates.

Table 2.4.1-1. Wavelength Ranges for Detector Segments

Channel	Segment A	Segment B
SiC 1	1090.9 - 1003.7	992.7 - 905.0
LiF 1	987.1 - 1082.3	1094.0 - 1187.7
SiC 2	916.6 - 1005.5	1016.4 - 1103.8
LiF 2	1181.9 - 1086.7	1075.0 - 979.2

Note to Table 2.4.1-1: The listed wavelength ranges cover the well characterized portion of the spectrum. The actual edge of the detector is as much as 1 Å different, however, the detector distortions are quite severe beyond the listed limits and have not been characterized. The dispersion direction of the two SiC channels is opposite that of the LiF channels. Both SiC1A and LiF1A refer to the same physical detector segment.

2.4.2 Effective Area

The combination of SiC and LiF coatings on the primary mirrors and gratings was designed to maximize the effective area across the whole FUV band. Since the reflectivity of LiF drops rapidly below approximately 1020 Å, the effective area changes significantly with wavelength. In addition, the gaps between the detector segments creates narrow bands (typically 10 Å wide) where the total effective area drops by as much as a factor of 2. Table 2.4.2-1 lists the derived on-orbit effective area at 10 Å intervals for each channel. Figure 2.4.2-1 plots the effective areas as a function of wavelength for the individual detector segments.

Table 2.4.2-1: In-flight Effective Area vs. Wavelength

Wavelength (Å)	Effective Area (cm ²)				Wavelength (Å)	Effective Area (cm ²)			
	SiC 1	SiC 2	LiF 1	LiF 2		SiC 1	SiC 2	LiF 1	LiF 2
910	4.6	0	0	0	1050	4.5	3.6	23.1	16.0
920	4.9	5.8	0	0	1060	4.0	3.0	22.2	14.4
930	4.9	6.2	0	0	1070	3.7	2.7	20.7	12.9
940	4.5	6.2	0	0	1080	3.3	2.5	17.6	0
950	4.3	6.4	0	0	1090	2.6	2.6	0	20.7
960	4.8	6.7	0	0	1100	0	2.3	19.2	21.3
970	4.6	6.8	0	0	1110	0	0	20.1	21.5
980	4.0	6.5	0	2.2	1120	0	0	19.7	21.1

990	2.8	6.6	3.4	3.0	1130	0	0	18.7	21.3
1000	0	5.6	8.5	5.8	1140	0	0	17.1	20.5
1010	4.5	0	17.7	9.4	1150	0	0	15.1	19.3
1020	5.1	3.8	22.9	12.1	1160	0	0	13.8	17.9
1030	4.9	4.0	23.2	13.6	1170	0	0	12.3	15.6
1040	4.8	4.0	24.4	15.8	1180	0	0	10.6	13.6

Note to Table 2.4.2-1: In order to avoid small scale variations, the effective areas quoted here are the averages of the values for three consecutive wavelengths, centered on the quoted one.

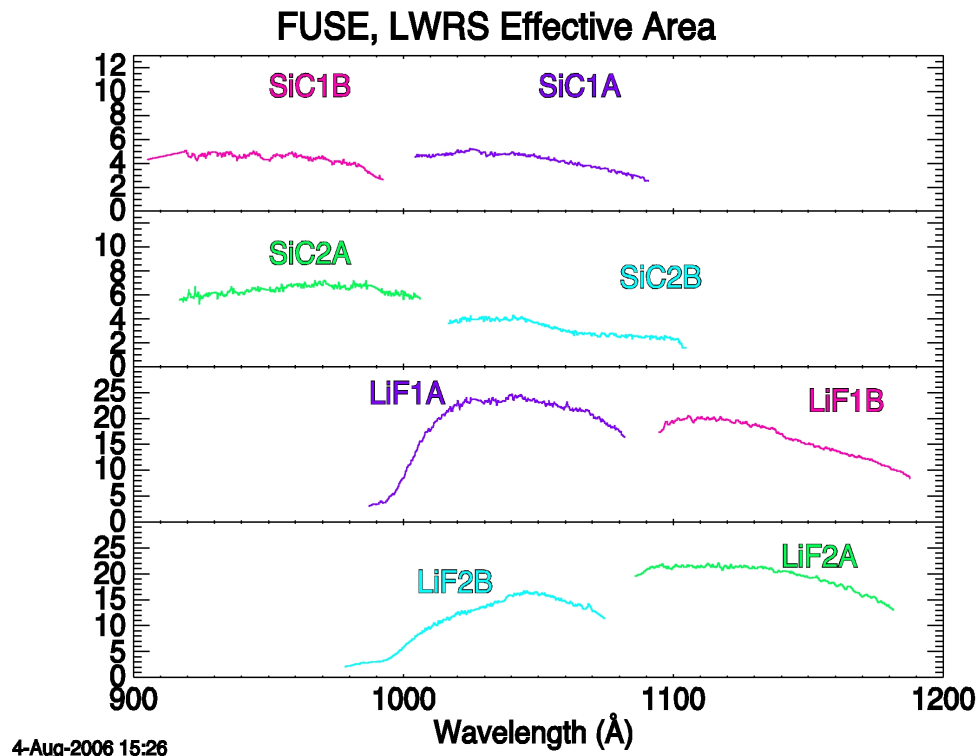


Figure 2.4.2-1 The in-flight derived effective area as a function of wavelength. Curves are shown for the individual detector segments. The effective area will change with time on orbit. (see text for details).

2.4.3 Spectroscopic Resolving Power

It has turned out to be difficult to assess the true spectral resolution of FUSE on-orbit for several reasons. It has been difficult to remove the smearing effects of the thermally induced image and spectral motions, and these motions affect HIST and TTAG data differently. Also, high signal to noise data are required, but uncertainties in the detector flat fields, and their effect on measured line widths, need to be assessed. Finally, most real sources do not have intrinsically narrow lines across the bandpass, making a thorough assessment difficult.

To date, the most quantitative assessment of resolving power is the following: The spectral resolving power was estimated by observing WD0439+466, a nearby white dwarf star exhibiting numerous narrow H₂ absorption lines in its spectrum. We obtained 15 histogram exposures. Each exposure was individually cross-correlated to remove the zero-point offsets due to image and spectral shifts, then co-added, resulting in a single, high S/N spectrum for each segment of each channel. Next, an astigmatism correction was applied to straighten the spectral line curvature (see next section), and the resulting image was collapsed in the spatial direction to form a 1-D spectrum.

We used the LiF1 data to construct a curve of growth for the H₂ lines. This allowed us to measure the thermal velocity parameter, $b = 3 \pm 1 \text{ km s}^{-1}$. This was deconvolved from the measured line widths to determine the intrinsic resolving power of the instrument. The result is $R = 20,000 \pm 2000$, and is nearly flat across the entire bandpass. This is the monochromatic resolving power. An observed line width will be the intrinsic line width convolved with the instrumental width, λ/bdR .

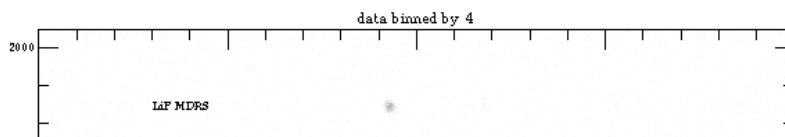
The data for this resolution estimate were obtained in the LWRS aperture in HIST mode. No detailed correction for image or spectral motion was therefore possible within each histogram, although the cross-correlation of the separate histograms removed the smearing that would otherwise be present in separate exposures. In addition, the 1×8 binning factor of histograms gives rise to a ~5-10% reduction in resolving power compared to time-tagged data. Thus, time-tagged exposures with good S/N may yield spectra with somewhat higher resolving power if care is taken in the data analysis.

2.4.4 Spectral Astigmatism

Although the FUSE gratings were created specifically to reduce astigmatism to a manageable level, the astigmatic height of FUSE spectra perpendicular to the dispersion direction is significant and variable as a function of wavelength. To recover the full spectral resolution, this astigmatism must be carefully characterized and removed from the data prior to collapsing it into a 1-D spectrum.

Two portions of an on-orbit spectrum recorded by flight detector segment 1A are shown in Figure 2.4.4-1. The top half of the figure shows x pixels 5800 to 7800, while the bottom half shows x pixels 11000 to 13000. Each of these regions covers about 12 Å. The target spectrum is visible in the LWRS aperture in both channels, and Lyman beta airglow is seen in both LiF (top figure) and SiC (bottom figure) channels through the HIRS and MDRS slits.

This image shows the variation in astigmatism as a function of both channel and wavelength, and also the tilt and curvature of the spectral lines. A dead spot is also visible at the top edge of the LiF spectrum near x=950 in the lower panel.



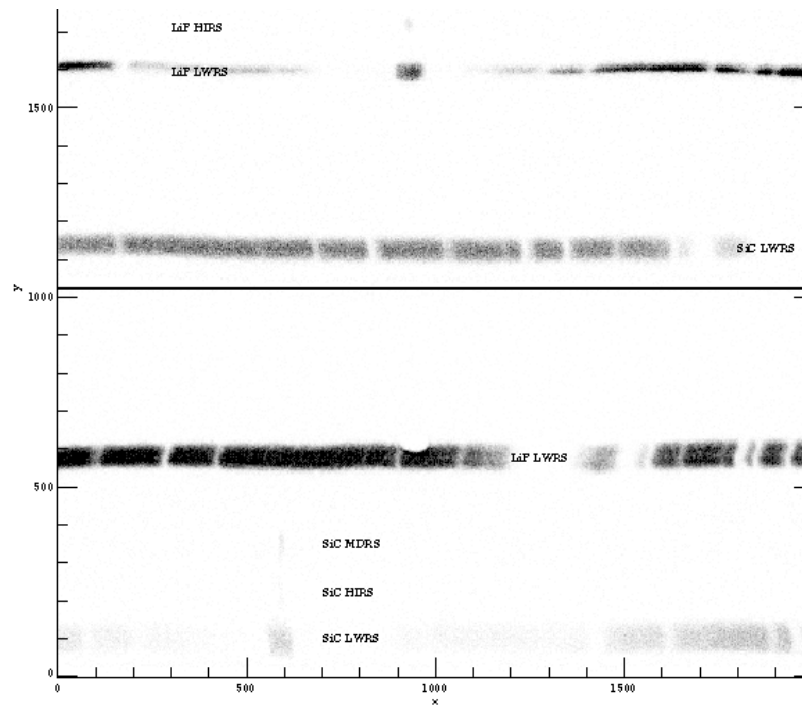


Figure 2.4.4-1. Two sections of an on-orbit spectrum on detector segment 1A. These regions were chosen to show Lyman beta airglow in the LiF (top panel) and SiC (bottom panel) channels.

The spectra discussed above are from side 1 of the instrument. For side 2, the order of the apertures is reversed from what is shown in Figure 2.4.4-1. The LWRS aperture is at the top of the image and the MDRS aperture is below the HIRS aperture. The LiF spectra are still imaged in the upper half of the segment, with the SiC spectra in the lower half. In addition, the y pixel sizes are larger than on side 1.

Although the holographic rulings allow for partial correction of astigmatic optical aberrations, the image of a point source still has a vertical extent of 200 to 900 μm (14 to 63 arcsec) on the detector. (Full extent of sources that fill the apertures can be as high as 1200 μm (100 arcsec). This vertical astigmatic height is a function of both wavelength and detector segment being considered. This means that virtually no spatial imaging capability is available, since the HIRS and MDRS apertures are only 20 arcsec in length (which projects to 220 μm on the detector). Only in the limited spectral regions near the minimum astigmatic heights in each spectrum will marginal spatial information (>10 arcsec) be derivable, and even then only with careful hand processing of the data sets.

Further information on astigmatic heights as a function of wavelength can be derived from [Figure 2.5.1-1](#).

2.5 Detectors

Two microchannel plate (MCP), double-delay line detectors are used in the FUSE instrument. The MCPs and delay line anodes are curved to match the Rowland circle. The active area of a detector must be approximately 170×10 mm in order to capture the full spectral range from a pair of gratings. This requires the use of two MCP stacks ("segments") in each detector. Each segment is 88.5×10 mm, and they are placed end-to-end in the long (dispersion) direction, with a ~ 7 mm gap between the stacks. Due to edge effects, the effective gap size is ~ 10 mm. The two detectors are displaced slightly in the dispersion direction so that no wavelength interval falls in the gaps of both detectors. Throughout this document the detector segments are labeled 1A and 1B (segments A and B on side 1), and 2A and 2B (segments A and B on side 2).

The photon event locations in each detector MCP segment are accomplished electronically and are digitized into $16,384 \times 1024$ pixels. On all segments, the X pixel size is $6.0 \mu\text{m}$. However, the Y pixel size is slightly different for the different detector segments. For segments 1A and 1B, the Y pixel size is $9.1 \mu\text{m}$. For segments 2A and 2B, the Y pixel size is 14.8 and $16.3 \mu\text{m}$, respectively. The detector resolution, however, is $\sim 25 \times 80 \mu\text{m}$ (i.e., the detector resolution is oversampled by ~ 4). The full instrumental resolution, including the optics and pointing jitter is about $50 \mu\text{m}$ (corresponding to $R = 20,000$; see [Section 2.4.3](#)).

Information for every photon event is packaged into a 4-byte packet and sent to the Instrument Data System (IDS) computer. Information in this packet includes the detector and segment number of the event, the X,Y location on the segment, and the pulse height of the event.

If the total count rate from the two detectors exceeds 32,000 counts/second, the bus between the detectors and the IDS cannot keep up, and events are randomly discarded at the detector. Spectral integrity is maintained, but photometric accuracy is compromised. The total number of photons detected (before discarding photons above the 32,000 count rate limit) is telemetered to the IDS from the detector. For count rates higher than ~ 15 -20,000 per segment, the dead-time correction begins to become important ($> 20\%$).

The total charge that can be extracted from the MCPs is a limited resource. High S/N observations of any target, bright or faint, deplete this resource and cause gain sags in the illuminated region of the detector, similar to that seen due to airglow line. [Section 3.5.2](#) describes the bright object limitations in greater detail.

Two sets of wire grids lie above the MCPs. A "QE grid", which improves the quantum efficiency of the detector by collecting photoelectrons generated by the MCP web, and a "plasma grid", whose job is to keep plasma in the earth's atmosphere from impinging on the MCP. Highly energetic particles will not be stopped by this grid and will result in either normal energy background events in the MCP or high energy events which are rejected by the pulse height discriminators in the detector.

A "stim lamp" is located just below the internal spectrograph baffles, and about 1 meter above each detector. This lamp is used in orbit as an aid in calibration.

Further details are given in [Appendix A, section A.5](#).

2.5.1 Detector Background

The background count distribution on the FUSE detectors is composed of two separate components. The first (typically referred to as the 'intrinsic' background) is an approximately uniform distribution of counts caused by the beta decay of ^{40}K in the MCP glass as well as energetic particles in the spacecraft environment. This component can vary depending on the level of solar activity and the details of the spacecraft orbit. While observations have shown that the orbital averaged intrinsic count rates can vary by a factor of 2 over periods of weeks or months, there appear to be only small changes during individual observations. The second component is caused by scattered light, primarily geocoronal Lyman alpha. This component produces well defined patterns of illumination on the detectors (see, e.g. Fig. 2.5.1-1) and varies substantially in strength during the orbit, with detector averaged count rates as small as 20% of the intrinsic background during the night and increasing to 1-3 times the intrinsic rate during the day.

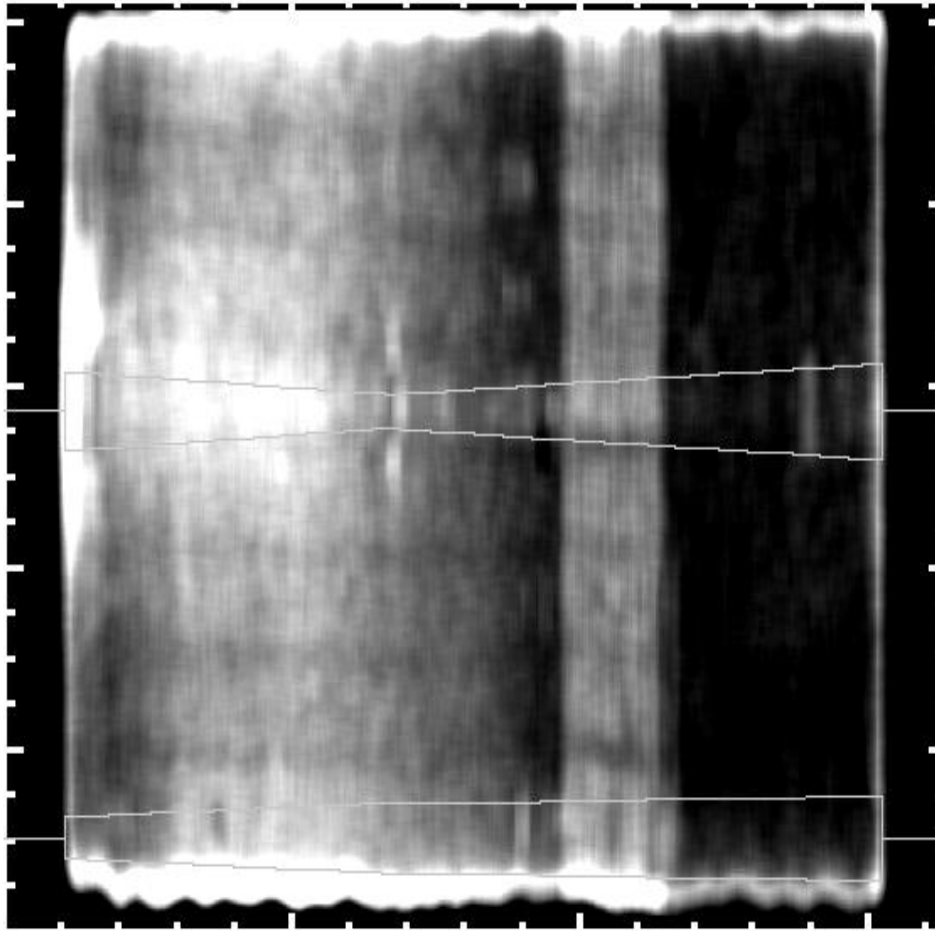
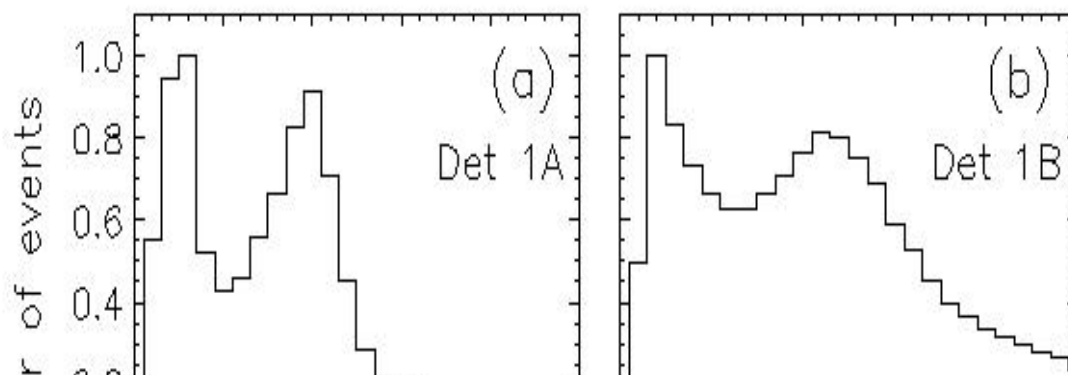


Figure 2.5.1-1. Image of the 1A detector obtained from a long (>200 ksec) exposure of empty sky taken early in the mission. The data has been smoothed by 200 pixels in the dispersion (X) direction and 20 pixels in the cross dispersion (Y) direction. Bursts and strong geocoronal emission lines have been removed before processing. The image illustrates the pattern of scattered light on the detector. The extraction window for the two low resolution apertures are also shown. Note that the SiC aperture (centered at $y=100$) is strongly affected by a background enhancement at the edge of the detector.

The number of electrons generated in the microchannel plate depends upon the type of initiating event, with the ^{40}K and energetic particles typically producing fewer electrons than normal photon events. A histogram of the number of electrons produced per event for a large number of events (termed the pulse height distribution - PHD) therefore shows a bimodal distribution (see Fig 2.5.1-2), with a strong, narrow peak at low values resulting from the intrinsic background superimposed on a much broader distribution caused by the photons.



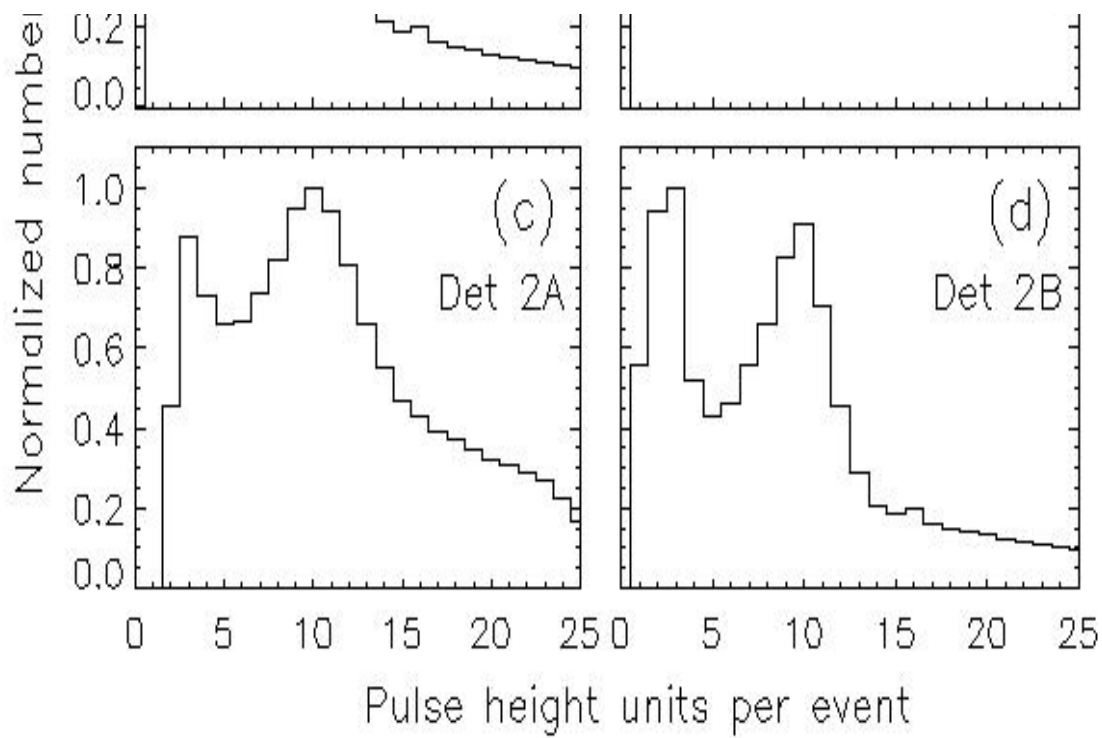
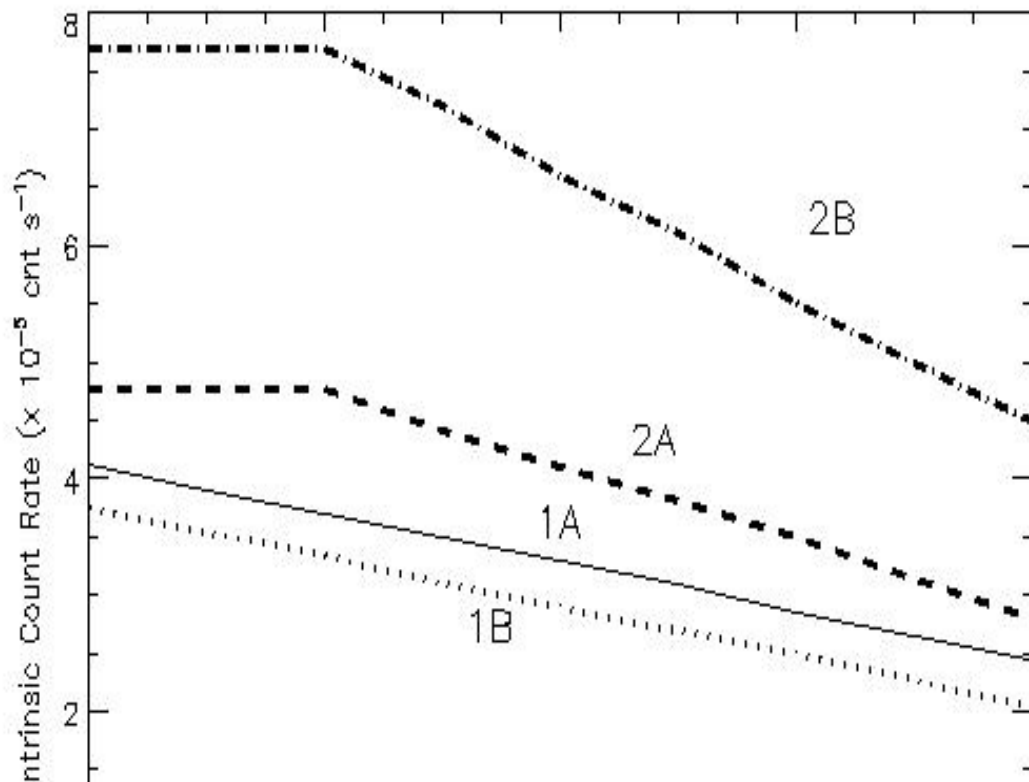


Figure 2.5.1-2. Example of the distribution of the number of pulse height units (each of which corresponds to about 10^6 electrons) produced during detected MCP events. This is commonly referred to as the pulse height distribution (PHD).

Thus, when reducing time-tag observations of faint sources where the intrinsic background is a substantial fraction of the source flux, it is often advantageous to eliminate all events producing a low number of electrons, since these are generated primarily by the background. This effect is shown in Figure 2.5.1-3, which shows the relation between the intrinsic count rate and the minimum accepted PHD count. Eliminating events with more than 4 pulse height units is not recommended, however, since you stand an increasing chance of removing photons originating in the source. Please see the CalFUSE web page for further details and updates.



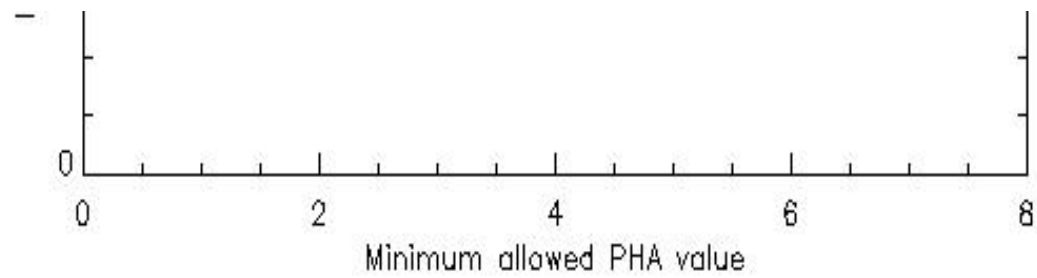


Figure 2.5.1-3. Measured count rate of the 'intrinsic' background component as a function of pulse height screening for the various detectors.

To illustrate the relative size of the FUSE background we plot in Figure 2.5.1-4 the slit integrated count rates for each of the low resolution apertures and compare it to the expected count rate from a source with a constant flux of $5 \times 10^{15} \text{ erg cm}^{-2} \text{ sec}^{-1} \text{ \AA}^{-1}$. The total background shown in the plot (solid line) illustrates a typical observation containing equal day and night contributions. As the fraction of night observing increases, the total background will approach the intrinsic rate (dotted line). The variation in the background with wavelength is caused by the varying astigmatic height of the spectrum as well as the structure of the scattered light distribution on the detector, while the variation in the source reflects the sensitivity function of the detectors.

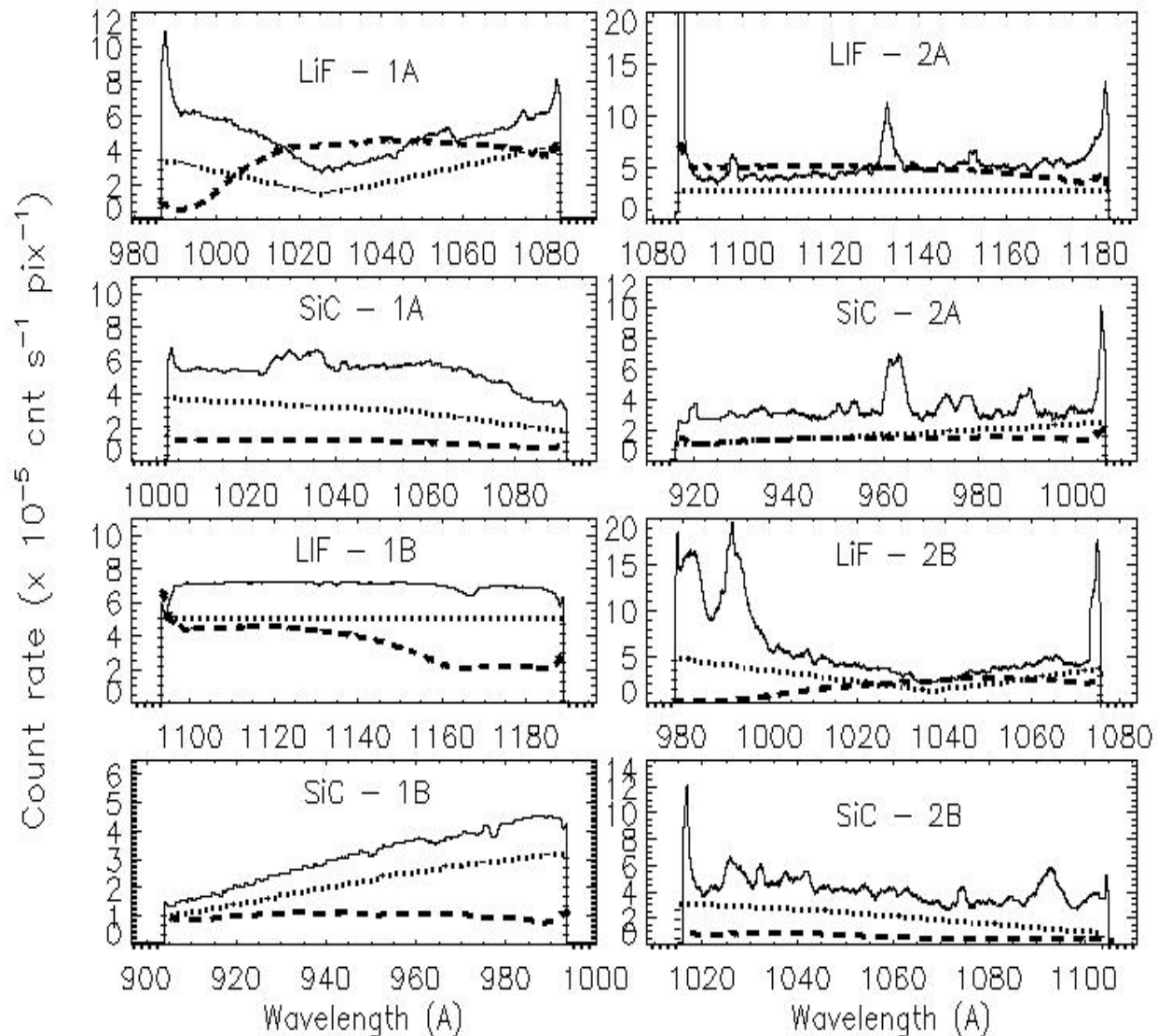


Figure 2.5.1-4. Count rates per pixel when integrated over the full astigmatic height of the spectrum. The solid line represents a typical background with both day and night contributions, while the dotted line is the expectation from the intrinsic background only. As the relative fraction of night increases, the solid line would approach

the dotted line. The dashed line shows the expected count rates for a source with a constant flux level of $5 \times 10^{15} \text{ erg cm}^{-2} \text{ sec}^{-1} \text{ \AA}^{-1}$.

The faintness of the background normally prevents us from accurately determining the form of the background distribution from an individual science observation. For this reason we have developed background models, which are a combination of a uniform intrinsic background image superimposed on a scattered light image which has been determined from long duration exposures of blank sky which have been taken throughout the mission (see Figure 2.5.1-1). The method used to derive the relative strength of these two components depends upon the type and quality of the data. For histogram data the background model is based on the exposure time and average values for the intrinsic and scattered light count rates. For TTAG data there are regions of the detector which directly sample the background and can be used to refine the background model. For short exposures, we use average values for the intrinsic background and scale the scattered light images until the total number of counts in a large background sample region of the model matches the counts over the same region of the observation. For longer exposures it is possible to determine the strength of both the intrinsic and scattered light components. To do this we subtract a constant, average intrinsic background (scaled by the exposure time) from the observation and compare the residual intensity variations along the dispersion (X) direction with those in a suitably scaled scattered light image. We then adjust the assumed value of the intrinsic background and repeat the analysis, noting whether the new model gives a better or worse fit to the observations. Continued iteration eventually converges to the most appropriate model. Finally, in some cases the measured background count rate is much larger than expected. Normally, this occurs when a contaminating source is present in one or more of the non-source apertures, e.g. when observing in comets, nebulae or crowded star fields. When this occurs the observed background is unreliable and a model is developed which is based only on exposure time. Comparison of several long duration observations has shown that the general structure of the scattered light distribution is relatively constant. Variations on the order of $\pm 15\%$ do occur over most of the data frame, while variations of $>30\%$ have been observed near the very edge of the detector. The distribution of scattered light also changes significantly when the high voltage of the detector is adjusted approximately every 6 months. For this reason the background distribution is being monitored and new calibration files are produced when large changes are evident. However, even with these precautions it is expected that the background model is unlikely to ever be determined to an accuracy of better than 10%. This implies that a source can be detected at the 3 sigma level when its flux is 30% of the background, while a maximum 10 sigma detection can occur when the source flux is equal to the background level. **Note, in this regime, high S/N ratios can't be obtained by increasing the integration time or reducing the resolution, since the observation is limited by the uncertainty in the background and not by the Poisson noise of the source.** In Figure 2.5.1-5 we present the expected S/N = 3 floor for FUSE, both with and without a scattered light contribution.

It is, in principle, possible to extend this faint limit to somewhat weaker sources by integrating long enough that the uncertainty in the on-chip determined background approaches its small scale variations, and performing a direct background subtraction from the data itself. However, this requires a fair amount of non-standard processing, in addition to a very long exposure. In addition, due to the gain sag seen along the LWRS spectrum such a background subtraction may still not be fully achievable.

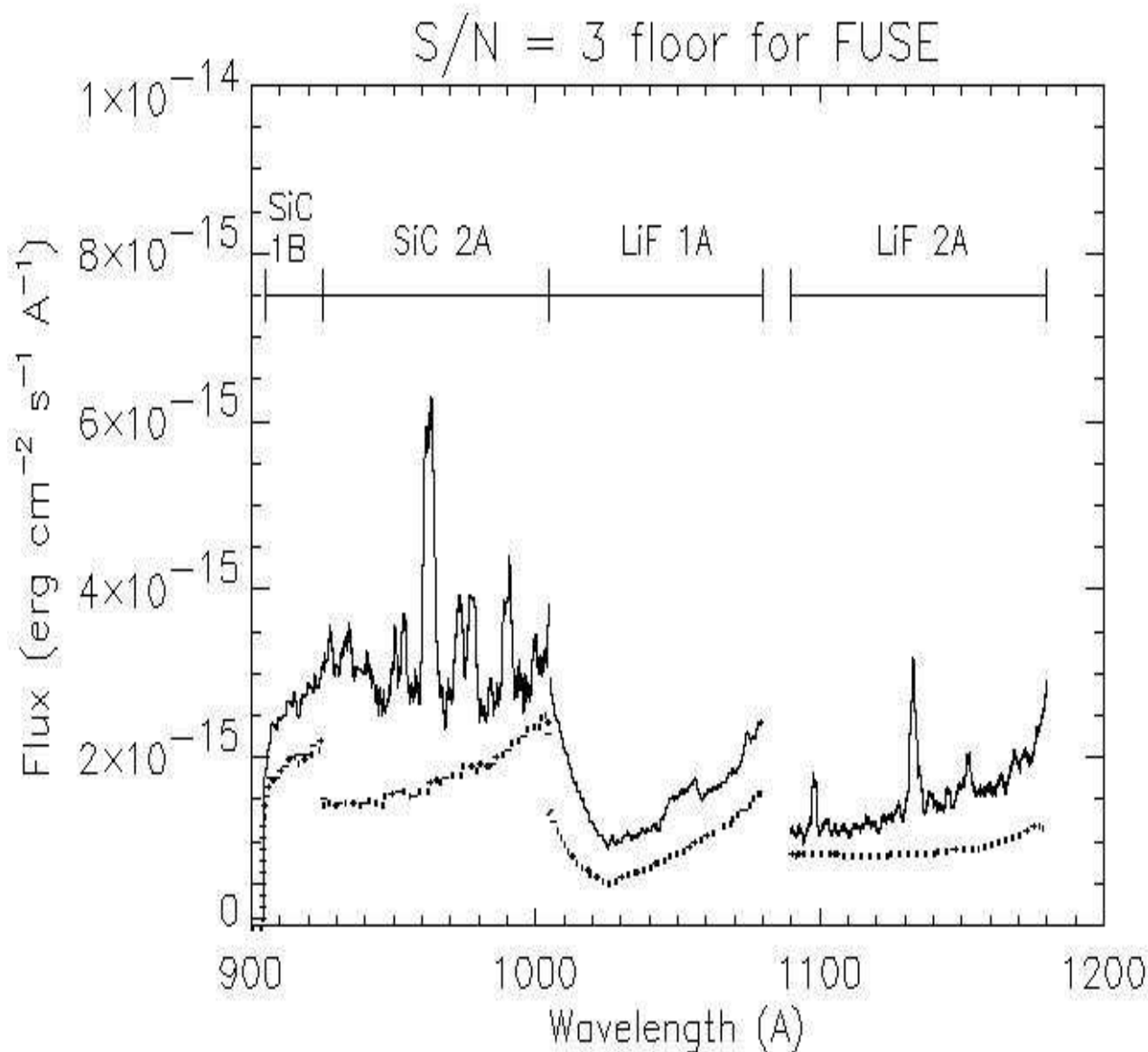


Figure 2.5.1-5. The minimum flux which can be detected by FUSE at a 3 sigma level, assuming that the background is only known to an accuracy of 10%. The dotted lines represent the expected fluxes when only the intrinsic background is important, e.g. when the observations are taken only at night. The solid line includes a scattered light component having the same intensity as used in Figure 2.5.1-4. The results for any given wavelength are taken from the best available detector, indicated at the top

of the figure.

2.5.2 Detector Flat Field

There are several important differences between flat-field images obtained with the FUSE detectors and those obtained with solid-state devices like CCDs. First, since the pixels in the double-delay line detectors are the product of read-out circuitry, they are not stable, fixed entities; i.e., their size and position can be affected by various factors, particularly temperature. Fortunately, FUSE data obtained on-orbit has shown that these thermally induced "drifts" in the detector are small. Second, because of distortions near the boundaries of MCP fiber bundles and non-linearities in the anode electronics (and, to a lesser extent, in the electron optics behind the MCPs), different areas of the photocathode can be mapped to a single read-out pixel. As a result, flat-field images for the FUSE detectors record both positional variations in QE response **and** distortions in the true photon event locations at the MCP.

Several of these distortions are illustrated in Figures 2.5.2-1 and 2.5.2-2. Figure 2.5.2-1 shows a portion of a prelaunch flat field image for detector segment 1B. The prominent hexagonal ("chicken wire") pattern is caused by the fiber bundles in the MCP. The diameter of a hexagon is about 0.6 mm (~0.6 Å) at the anode. A small, circular region of low response is also visible near the right-hand side of the image. This is due to a number of blocked pores, or possibly a small hole in the MCP.

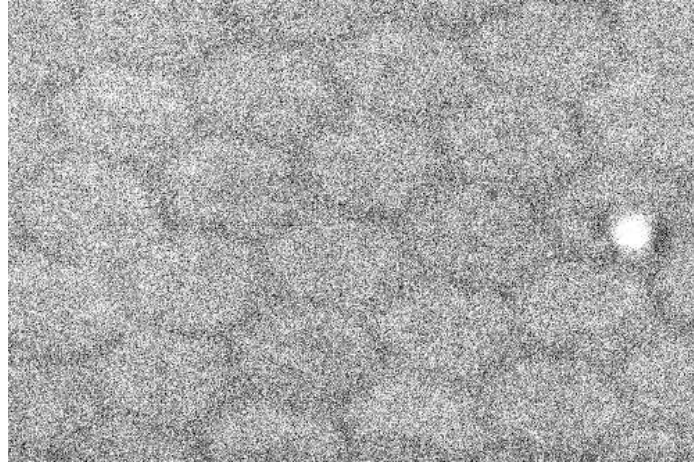


Figure 2.5.2-1. Flat field image of a region on segment 1B. This image is $3000 \times 3333 \mu\text{m}$ (500×333 pixels) in size. Darker colored areas have higher intensity. The contrast has been enhanced to show the "chicken wire" pattern, which is typically a 10-20% effect across the fiber bundle boundaries.

Figure 2.5.2-2 shows a section of the flat field for segment 2B. Several features are evident. First, there are spots of low sensitivity that range in size from several pixels up to many resolution elements across, some of which appear to be "edge brightened." The edge-brightened spots are likely due to a blocked pore at the back of the MCP stack, which distorts the electric field and causes the charge to be redistributed to a region around the pore. Detector 1 has several large dead zones in it, only a few of which coincide with the positions of the spectra. Unfortunately, detector segment 2B has many smaller blemishes that compromise localized regions of spectrum to varying degrees.

Fig. 2.5.2-2 also shows a pronounced moiré pattern of nearly vertical ripples. This pattern is the dominant component of the fixed-pattern noise. It is characterized by a period of about 9 pixels in X (i.e., a bit larger than a resolution element) and amplitude of 15% in the worst places, but below detection thresholds in others. The pattern is thought to be caused by interference effects between the glass plates of the MCP stacks. It is present on all detector segments, but is particularly bad on 2B.

Preliminary characterization of all these forms of fixed-pattern noise suggests that they are stable in time. Although the hexagonal and moiré patterns are caused by unequal mappings between area on the photocathode and read-out pixels rather than true sensitivity variations, the mappings are all one-to-one. Consequently, these signals can in principle be removed from scientific data by division of a suitable flat-field image.

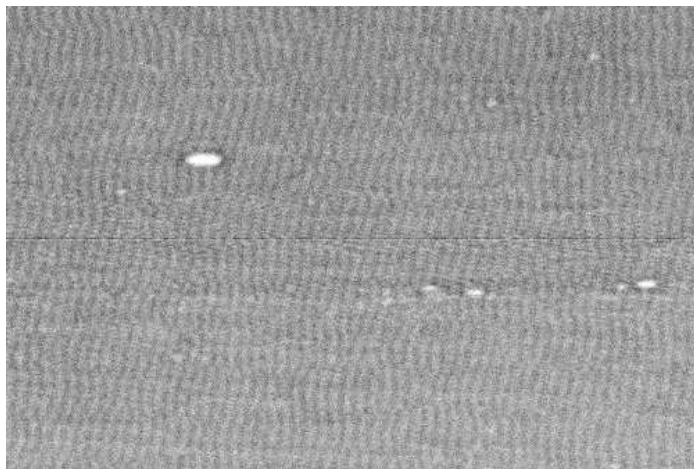


Figure 2.5.2-2. Flat field image of a region (500×333 pixels) on segment 2B. Darker colored areas have higher intensity. The image contrast has been enhanced to show the moiré pattern which is a ~10% effect.

Unfortunately, the flat field images obtained during prelaunch calibration do not remove fixed-pattern noise effectively. Since observations of the stim lamps are compromised by shadows from the wire grids, there appears to be no way to obtain a full, two-dimensional flat field image from data obtained on-orbit. Instead, considerable effort has been expended to derive one-dimensional flat field information from observations of FUV-bright subdwarfs and white dwarfs. This approach appears to be capable of removing detector artifacts spread over at least 30 pixels (i.e., ~3 or more spectral resolution elements). However, thus far efforts to remove the small-scale moiré pattern have not been successful, primarily because of unexplained shifts along the dispersion direction in the derived flat fields. As a result, the fixed-pattern noise responsible for limiting the S/N in observations of bright targets is not being corrected.

At present, the best way to combat fixed-pattern noise on these small scales is to make use of the movement of the image across the detector due to the combined effects of pointing jitter and mirror motion. In some cases, it may be desirable to augment these motions with deliberate movement of the source across the LWRS aperture, particularly if spectral features in the guide channel (generally LiF1) are of special concern. Since spectra from different exposures of an observation fall on different parts of the detector, they need to be aligned in wavelength (i.e., shifted in pixel space) before they can be added. This "shift + add" technique is quite effective in averaging over small-scale fixed-pattern noise; see, e.g., [Sonneborn et al. 2002, ApJS, 140, 51](#), who show that substantial enhancements in the final S/N can result for spectra of bright sources.

2.5.3 Detector X-Walk

The x position (~wavelength) of a photon falling on the FUSE detector is determined by measuring the time it takes for the resultant charge cloud from the MCP to propagate to the two ends of the delay line anode. The algorithm used for determining the time difference is a function of the shape of the pulse on the anode. Since the propagation along the delay line can change the shape of the pulse, particularly in cases where the pulse size (pulse height) is low, the calculated location of an event can depend on the pulse height of the event. The exact details of this variation, (called "walk") depend on where the event is on the detector, and how the electronics are optimized.

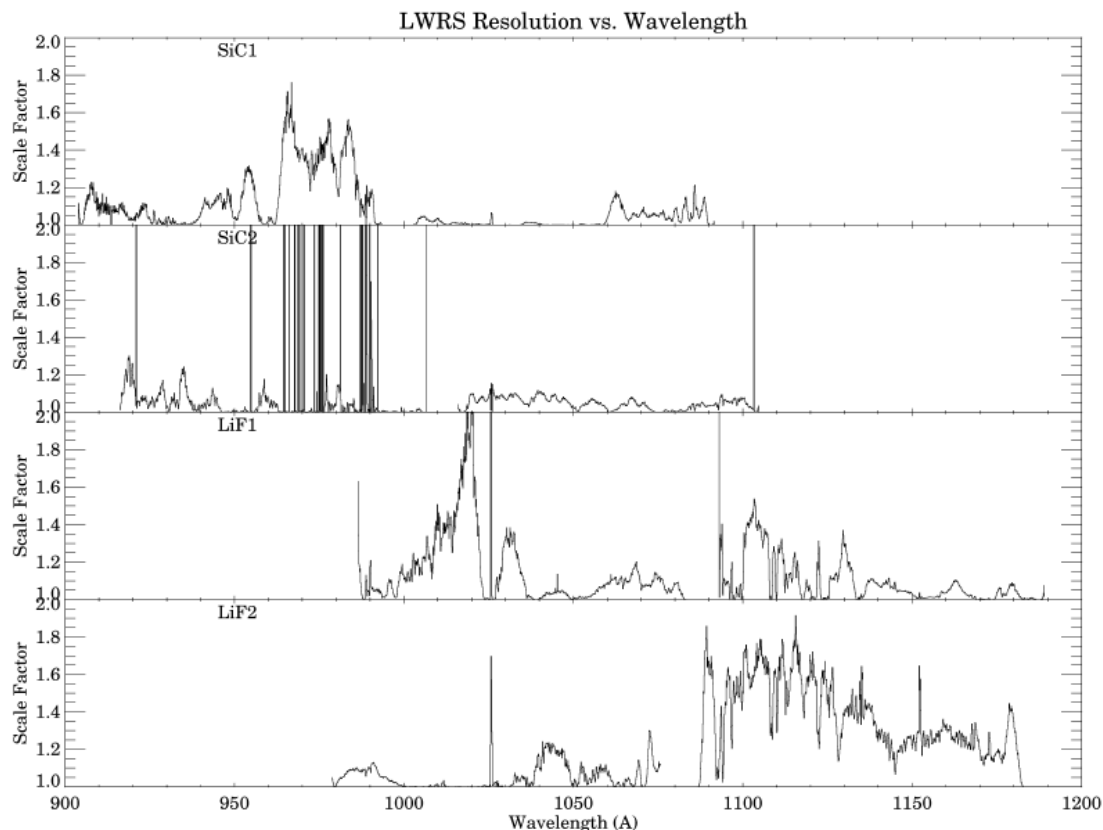
Early in the mission, the modal gain (most common pulse height value) of the detector was relatively constant across each segment. With exposure to photons, however, the gain has dropped, and variations across the detectors have developed. This is an inherent characteristic of MCPs and was expected. After many months of exposure, certain regions of the detector (e.g. the locations of bright airglow lines in the LWRS, which are always being illuminated) have collected many more events than others. Thus, there is a variation in gain with position, and therefore a distortion in x which changes with time and location on the detector. In order to alleviate this problem, the detector high voltage (HV) is periodically raised, which helps to minimize the gain variations. We performed the first such HV increase at the end of January, 2001 and have followed up with further increases about every six months.

The effect of the walk variation is a slight blurring of the spectra, and thus a slight loss of resolution, which is position (wavelength) dependent. For data acquired in TTAG mode, the CalFUSE pipeline corrects the x location of events using an empirical walk correction. For HIST observations, where the pulse height information is not available a statistically based correction is applied, which partially addresses the problem.

The existence of the gain sag by itself is not a reason to request an aperture other than the LWRS for low count rate targets, since the pipeline corrections minimize the impact on the calibrated data.

To compensate for the gain-sag and the consequent x-walk, the FUSE project has routinely raised the high-voltage (HV) on the detectors as needed. However, we have found that for detector 2A we can not raise the HV further. As the gain-sag progresses, this causes some areas of the detector to have significant parts of the pulse-height distribution fall below the minimum detectable level. This then becomes equivalent to a localized loss in sensitivity. As most areas of large gain sag corresponds to terrestrial air-glow lines, and are thus relatively narrow, these sensitivity losses can be compensated for by performing FP_SPLIT observations. Hence, for observations for which small scale data on the 2A detector is required - particularly close to known, bright air-glow lines - users should consider requesting FP_SPLIT observations and/or the MDRS aperture.

Additionally, it should be noted that for HIST observations, where walk corrections cannot be exactly calculated, an increased spectral "smearing" is unavoidable for many regions of the spectrum (Figure 2.5.3-1).



4-Aug-2006 12:16

Figure 2.5.3-1. Estimated degradation for the spectral resolution, for HIST mode observations acquired in the LWRS aperture. In HIST mode, the X-walk corrections are not fully compensated for in the pipeline processing and the effective resolution is therefore lowered. For HIST mode in the LWRS aperture the achievable spectral resolution can be estimated by dividing the nominal resolving power $R=20,000$ by the Scale Factor given in this figure. The structure in SiC2 between 950-1000Å is due to analysis artifacts; an updated figure with these artifacts removed is expected in the near future.

2.5.4 Worms

Dark horizontal stripes are often seen in two-dimensional detector images of FUSE spectra. The features, commonly referred to as "worms" because of their shape, can appear in spectra obtained through all three FUSE apertures (LWRS, MDRS, and HIRS). They have been observed to move during an observation, and their exact location depends on the Y position of the target in the aperture. The most famous worm appears in LWRS LiF 1B spectra and adversely affects the absolute flux calibration of that channel.

These worms are due to shadowing by the QE grid wires at locations where the secondary focus falls above the detectors and close to the location of the wires. Work is under way to correct, or compensate for the worm in the CalFUSE processing. At present, the worms do cause severe impacts on the local flux calibration. To what extent the work under way will fully alleviate these problems is at present unknown.

2.6 Fine Error Sensor Cameras

Each of the two LiF channels has a Fine Error Sensor (FES) camera that images the 19×19 arcmin field in the neighborhood of the science target. Visible light is directed to the FES CCD from the mirrored front surface of the FPA. The FES determines the centroids of up to six guide stars in the field with an accuracy of 0.2 arcseconds and sends this information to the Instrument Data System (IDS) typically once per second. This results in a satellite pointing stability of 0.3 arcseconds (rms).

In-orbit checkout soon after launch showed FES-A to be superior in performance to FES-B, and it was initially designated the primary FES. After intermittent problems arose with FES-A during the spring and early summer of 2005, FES-B was designated primary FES in July 2005. FES-A monitors light reflected from the LiF1 FPA. Similarly, FES-B monitors light reflected from the LiF2 FPA. Hence, the LiF channel off of which the active FES works will, by definition, stay fixed on the FPA.

In order to improve the image quality in FES-B, while keeping the FUV optics focused, the LiF2 FPA has been moved to a position that is offset from the focal plane of the LiF2 primary mirror. As the FUV beam is not at its minimum lateral extent at this position, some light is lost when using the two smaller apertures (see section 2.1, above).

For guiding, the practical limiting magnitude of the FES is $V \sim 13.0$, or 14.0 if a standard 2-s update parameter is invoked. This is sufficient to find guide stars in the vast majority of situations. However, given uncertainties in listed magnitudes of HST Guide Star Catalog stars (and uncertainties in star colors), the $V = 13.0$ boundary is gray. If only stars near or below this limit are available, we must still be wary about using them. In some fields near the galactic poles it may be necessary to schedule observations at a particular time to ensure availability of guide stars. Thus, guide star availability can be a driver of scheduling in certain cases.

The imaging properties of the FES are modest. The stellar point spread functions are typically 5 arcsec FWHM, depending on field angle, color, and mirror-to-FPA focus position. Nevertheless, an image of the field (with the target either in or out of the aperture as requested by the investigator) will routinely be provided to users to confirm that the proper target was acquired. We expect the photometric calibration of the FES to be good to < 0.1 mag.

Each FES has a three-position filter wheel, containing a clear, color (V for FES-A, R for FES-B), and neutral density (ND6) filter. However, we are currently using only the clear position since the other filters are not needed for normal operations. Further details of the FES cameras is available in [Appendix A, section A.6](#).

2.7 Instrument Data System

The Instrument Data System (IDS) is a redundant, programmable processor (68020 with floating point coprocessor) that controls the FUSE instrument. (A "redundant" system contains a primary processor and a backup processor.) Only one of the two processors is powered on at a time. The active IDS processor communicates with the spacecraft subsystems (for example, the spacecraft attitude control system) over a data bus with a maximum data rate of ~250 kbps. Instrument science and engineering data are sent to the spacecraft solid-state recorder over this bus. Science data are allocated up to 120 kbps of the bus traffic. The IDS also receives a 1 Hz signal from the spacecraft that is used to synchronize the IDS clock with the spacecraft clock to an accuracy of ± 5 millisecond. The IDS controls all slews, target acquisitions, data collection, and instrument health and safety functions by means of on-board scripts prepared by Mission Planners and the Mission Operations Team.

The IDS communicates simultaneously with all instrument subsystems, and is responsible for controlling all instrument functions, including thermal control, actuators on the mirror assemblies and FPAs, and detector and FES operations. It accepts data from the FUV detectors and FES, and packetizes the data for transmission to the spacecraft solid-state recorder. The IDS also collects "housekeeping" telemetry (temperatures, voltages, etc.) from these subsystems, packetizes them, and sends them to the recorder.

The IDS plays a crucial role in the pointing performance of the instrument. After a slew to a new target field, the IDS processes the FES image of this field, and determines the boresight pointing based on comparison with a star table uplinked from the ground for each separate observation. This measured pointing is sent to the spacecraft Attitude Control System (ACS) to update the current pointing and the spacecraft is slewed to the desired target position. Once the FES acquires guide stars (pre-selected from the field star table for each observation), it begins sending centroid information to the IDS for the guide stars. The IDS computes the measured quaternion (pointing vector) once every second and sends it to the ACS to maintain pointing stability. Guiding is terminated prior to each spacecraft occultation, but as long as guide stars have been acquired prior to entry into the South Atlantic Anomaly, guiding can proceed through the SAA period (if the target is unocculted).

3. Planning Observations

Sections 1 and 2 of this *Guide* contain background information needed for planning FUSE observations. In this section we discuss several issues that have to be considered while writing a FUSE observing proposal. In Section 3.1 we provide a summary of these issues, which are then described in more detail in subsequent sections.

3.1 Brief Guide for Proposers

When writing a Phase 1 proposal, or providing detailed information in Phase 2 forms for accepted proposals, one has to choose which aperture to use, whether the source flux is in an acceptable range for FUSE observations, what exposure time is needed to obtain the desired signal to noise, whether time-tag observations should be requested and whether offset stars are needed for target acquisition. At the Phase 1 stage, it is also useful for proposers to understand the scheduling process at a rudimentary level so they may estimate how constrained their observations are.

3.1.1 Choosing Apertures

The three apertures supported are the LWRS (30"x30"; 100% throughput), MDRS (4"x20"; 98% throughput; 70% for LiF2) and HIRS (1.25"x20"; 85% throughput; 15% for LiF2) apertures.

- **LWRS:** This is the default aperture. For a point source, the spectral resolution is as high for observations using the LWRS as for those using the MDRS. The channel drifts (see Sec 3.6.7) are smaller than the aperture size so shorter wavelength coverage (SiC channels) is routinely obtained.
- **MDRS:** When the desired target is in a crowded field, or has a UV bright companion within 30", the MDRS may be useful in keeping out contaminating objects. The MDRS is also useful for obtaining higher spectral resolution for extended objects that fill the slit, or for minimizing airglow contamination. Channel drifts are of order the aperture width, but keeping the SiC channels aligned is possible. For bright targets observations (HIST mode) where data in regions close to any of the brighter terrestrial airglow lines are of interest, MDRS should also be used.
- **HIRS:** This is used for the same reasons as the MDRS. In addition it can provide higher spectral resolution for point sources. However, channel drift problems will be severe and only LiF 1 coverage is guaranteed.

3.1.2 Flux Range

Bright Limit: The microchannel detectors have a finite reservoir of charge that can be extracted. Exposure to bright sources depletes the charge and will result in rapid decay of the detector sensitivity. Therefore it is of paramount importance that the proposer makes sure the requested target(s) have fluxes that are below the bright limit. The brightness limit for FUSE observations is $1 \times 10^{-10} \text{ erg s}^{-1} \text{ cm}^{-2} \text{ \AA}^{-1}$ at all wavelengths (this applies to continuum as well as emission line targets).

There are special modes for observing targets that are brighter than this limit by a factor of a few. Due to the lower effective area in the SiC channels and the lower throughput in LiF2 HIRS, the brightness limit for SiC only or LiF2-HIRS only observations is $5 \times 10^{-10} \text{ erg s}^{-1} \text{ cm}^{-2} \text{ \AA}^{-1}$. Observation of such targets (even if approved by the TAC) is subject to clearance by the project based on detector safety considerations. See Sec 3.6.2. for details.

For cycle 8, no over-bright targets, beyond the above raising of the limit in SiC ONLY and LiF2-HIRS ONLY limits, will be allowed.

Faint Limit: The detector background level makes it difficult to get useful signal to noise for targets that are fainter than $5 \times 10^{-15} \text{ erg s}^{-1} \text{ cm}^{-2} \text{ \AA}^{-1}$. However, long exposures with careful and non-standard background subtraction can be used to study fainter objects. See Sec 3.6.3 for details.

3.1.3 Observing Modes and Observation Types

All observations are done in either time-tagged (TTAG) or histogram (HIST) mode. TTAG (time-tagged) mode is used when the expected count rate is below 2500 events/sec. Time resolution of 1 second is the default. Higher time resolution (up to 8 ms) can be requested if the science demands it. HIST (histogram) mode is used for high count rate observations. Otherwise, the on-board data recorders would fill up and data would be lost. Because of high data volume the number of HIST exposures that can be obtained between ground station passes is limited.

The standard observing procedure is the default for all targets. Special requests for SNAPSHOTS, FOCAL PLANE SPLITS, FES IMAGES, and a few non-standard (and usually unsupported) configurations can be made. Details about these different types of observations are given below in Section 3.2.

3.1.4 Signal to Noise and Exposure Time Calculations

The maximum achievable signal to noise for a normal observation is about 30. FP-SPLITS may be requested when higher S/N is essential. The exposure time required to achieve a given S/N can be calculated using the on-line exposure time calculator (ETC; http://fuse.pha.jhu.edu/support/tools/exposure_time_tool.html). The steps for the calculation are given in Appendix C of this document. For bright (HIST) targets where data in segments other than LiF2 are required, the requested exposure time should be doubled from that given by the ETC to compensate for alignment shifts.

3.1.6 Target Acquisition

For most targets, acquisition is routine (and needs no specific input from the proposer). However, for extended objects (galaxies, nebulae) the proposer is required to provide a UV bright OFFSET star within, at most, 2 degrees of the target (a maximum distance of 30 arcmin is strongly preferred).

3.1.7 Scheduling Considerations

Details of the scheduling are not of great importance to the proposer, but it is necessary that he/she be aware that several observations are considered "constrained", either because they are time specific (targets of opportunity, monitoring observations) or the period of visibility of the target over the cycle is small (less than 2 weeks total). In a given cycle, only a limited number of such constrained observations are possible. Scheduling and time critical observations are discussed below in Sections 3.4 and 3.7.

3.2 Observing Modes

The FUSE instrument has a simple design with few observing modes. In fact, the user normally does not have to worry about choosing most of the modes described below; the correct mode of observing will be derived from the Phase 2 proposal information (based on target flux and the desired S/N and spectral resolution). The default modes are described below, and the user has the option of requesting a non-default mode of operation on the Phase 2 form. *Requests for non-default modes of operation will be considered only if it can be demonstrated that the quality of the science will be significantly improved.*

3.2.1 Time Tag (TTAG)

Every photon event recorded by the detectors is sent to the Instrument Data System (IDS; the instrument computer). The information recorded for each event includes the X and Y location of the event on the detector and the pulse height of the event. The detector itself does not record the time of arrival of each photon. Photon events from all four detector segments are sent to the IDS over two RS-422 serial lines. The maximum rate at which the IDS can process photon events in TTAG mode is $\sim 8,000$ events/sec. *The IDS does not time-tag every photon event.* Instead, the IDS inserts time words into the data stream at a nominal rate of once per second (adjustable). Hence, the relative accuracy of photon arrival times when observing in time-tag (TTAG) mode, is 1 second. This is more than adequate for computing Doppler shifts or determining "good time intervals" for a dataset.

What are the advantages of TTAG mode? Observing in TTAG mode allows the data to be stored with the full detector sampling ($6 \mu\text{m}$ in X and $9.1\text{--}16.3 \mu\text{m}$ in Y), which will allow the highest spectral resolution to be derived from the data (after removing spectral astigmatic curvature and thermally-induced spectral motions). If data were taken too close to the South Atlantic Anomaly (SAA), resulting in undesirable background levels, the data set can be edited to remove data from the bad time period. In addition, the data through all apertures are saved and sent to the ground as part of the observation dataset. Finally, when the target is faint, TTAG mode uses memory very efficiently since most detector pixels do not contain any events during an exposure. A further advantage is that TTAG mode observations can be corrected for the gain-sag induced detector walk (see section 2.5.3)

What are the disadvantages of TTAG mode? The only real disadvantage is one created by onboard storage limitations for brighter targets, in combination with the sporadic nature of ground station contacts. The spacecraft solid state recorder has space for only ~ 120 MBytes of scientific data. In comparison, a bright star with a photon event rate of 7,400 counts/sec would require ~ 60 MBytes of storage for a single 2000 sec exposure! Consequently, the expected photon event rate from the target is used to determine the observing mode.

The presence of considerable spectral motion on the detector, characterized on-orbit, has made it desirable to observe targets in TTAG mode whenever possible. Hence, for event rates < 2500 counts/sec (corresponding to a flat spectrum source with flux of $\sim 8 \times 10^{-12} \text{ erg cm}^{-2} \text{ sec}^{-1} \text{ \AA}^{-1}$ in the LWRS aperture), TTAG mode is the default observing mode. For rates higher than this, spectral image (HIST) mode is used by default (see below). There is obviously a "gray" zone where one could use either TTAG or HIST mode (pending downlink capability to offload the solid state recorder), and the user is allowed to request TTAG mode at somewhat higher count rates if sufficient justification is provided. (This requires special scheduling of the observation to ensure downlink is available at the proper time.) Even objects with expected count rates near the nominal count rate boundary must be scheduled near ground station passes to prevent overflowing the solid state recorder.

Because of these issues, it is important that reasonably accurate fluxes and count rate estimates be made available for high-count-rate TTAG observations. For example, if a target with an expected count rate of 2500 cts/sec was underestimated by 30%, 6 - 8 Mbytes more memory would be required *per orbit* of typical observation! This could adversely impact both the observation of that target and potentially targets downstream in the plan since data collected after the recorder is full will be discarded. Hence, if a target has a TTAG expected rate, but an uncertain flux level, the observation may still need to be done in HISTogram mode.

3.2.2 Spectral Image or Histogram (HIST)

When the expected count rate is higher than 2500 events/sec, the IDS is configured by default to bin the data in its memory to form a spectral image, or histogram (HIST). Obviously, in doing so, the time-tagged nature of the events is no longer preserved during the exposure. Hence, it is not possible to edit spectral images to remove data obtained during periods of high background.

One advantage of observing in HIST mode is that higher data rates are supported. In HIST mode, the IDS can process photon event rates from the detector at rates up to 32,000 events/sec (corresponding to a flat spectrum source with flux of $\sim 8 \times 10^{-11} \text{ erg cm}^{-2} \text{ sec}^{-1} \text{ \AA}^{-1}$), which is very close to the stated brightness limit.

Although HIST mode helps relieve the data storage problem for bright targets, it does not solve it altogether. At full resolution, each detector segment is 16384×1024 pixels in size, resulting in spectral images which are 32 MBytes each, or 128 MBytes(!) for all 4 detector segments. Furthermore, spectral images are built up in IDS memory before sending them to the spacecraft recorder, and the IDS has only ~ 35 MBytes of memory! Consequently, we cannot store photon events for the whole detector in HIST mode. Instead, only the area of the detector containing the spectra taken through the primary aperture are stored in memory. The heights of the spectra due to astigmatism are $\sim 1200 \mu\text{m}$ at worst; hence, the storage requirement for a single HIST exposure at full detector pixel sampling would be ~ 29 MBytes. Taking spectral images of this size are not supported for general observing.

In practice, the curvature of the astigmatic line spread functions is not severe enough to require high frequency sampling in the Y direction (i.e., perpendicular to the dispersion). Consequently, for more efficient memory usage, the default spectral image mode is to bin the data by a factor of 8 in the Y direction and 1 (no binning) in the X (dispersion) direction. This reduces the size of a spectral image to < 5 MBytes per exposure. This binning does not affect the resolution at all for most wavelengths, and degrades the nominal spectral resolution by a few percent at worst.

Even with a size of ~ 5 MB per exposure, observing in HIST mode presents several other problems. The maximum Doppler shift (when observing close to the orbital plane) is $\pm 7.5 \text{ km s}^{-1}$, which is comparable to the nominal spectral resolution ($\sim 10 \text{ km s}^{-1}$). Likewise, the thermally-induced spectral motions described earlier would also smear out HIST data if left unchecked. Consequently, FUSE spectra must be corrected for these changing shifts at the time of the exposure. The only way we can minimize the smearing of HIST data is to take

exposures that are short enough so that the smearing is small compared to the spectral resolution. To simplify mission planning, a fixed number (4) of HIST exposures are typically made per orbit. (In special cases where resolution is of utmost importance, this number can be increased, with an additional load on memory usage.) This limits the Doppler and other smearing to typically $< 5 \text{ km s}^{-1}$ per exposure.

FUSE is supported by a primary ground station in Puerto Rico, which means that there is a period of about 12 hours every day when there is no opportunity to downlink stored science data. During this ~7 orbit communications "blackout", the total amount of science data accumulated must be less than 120 MB. Therefore, we cannot observe continuously in HIST mode for the whole blackout period. *Data storage space is a limited resource, and the number of HIST mode observations that can be done per day are therefore similarly limited.* Managing the available recorder space is a high priority job for mission planning, and can be a limitation to on-orbit operations.

3.2.3 Snapshots

Snapshots are short exposures scheduled well in advance of a primary science observation. There are at least three reasons that one might request a snapshot of a target:

- The target is predicted to be near the bright flux limit for FUSE, but considerable uncertainty in the flux level exists; attempting a nominal science exposure without knowing the true flux may damage the instrument (i.e., a safety issue).
- The target is expected to be faint but the FUV flux is unknown or uncertain. Hence, a "preliminary" observation for a fraction of the total desired time is requested first to verify flux levels before investing a large block of observing time.
- A number of targets need to be observed for a brief time, so that some subset of the total can be scheduled for longer follow-up observations.

Requests for these types of snapshots can be made in the Phase 2 template file using one of two special requirement keywords; the first case above would invoke SAFTSNP (Safety Snap) and the second and third cases would use the SNAP special requirement. (See the [Phase 2 Proposal Instructions](#) for more information.) In either case, the use of snapshots implicitly assumes a delay of at least 30-day before a follow-up observation can be scheduled. This is to allow time for the user to receive and analyze the snapshot data, make appropriate decisions, and report the results back to FUSE Mission Planners. Although the follow-up observation may appear on a long-range plan, the observation will NOT be allowed into a short-term schedule until FUSE Mission Planners receive word from the user as to the observed flux. (In the case of SAFTSNPs, both the user's analysis AND confirmation by a member of the FUSE Science and Operations team are required before the follow-up observation.) Faster turn-arounds will be considered on a case-by-case basis.

The use of snapshots should be used sparingly, since they lead to inefficient observing scenarios, especially for bright targets. Observing a target once to determine the flux and then returning later for further exposures incurs the extra overhead of repeated target acquisitions. The user should also note that observations of bright UV sources, with their potential for damaging the microchannel plates, may need to be delayed until later in the mission when special operating procedures have been developed fully (see [Section 3.5.2](#)). Time for any SAFTSNP exposures should be included in the Phase 1 and Phase 2 time requests at a rate of 2000 seconds to account for the large overheads involved in this mode.

3.2.4 Focal Plane Splits

The FUSE detectors suffer from a fixed pattern noise (see [Figure 2.5.2-1](#)). Due to the astigmatism in the instrument, however, a typical resolution element is spread over several hundred detector pixels, thereby somewhat mitigating the fixed pattern noise. Achieving the highest possible S/N (consistent with photon statistics) requires the removal of the remaining fixed pattern by one means or another. The most formal of these methods is called "focal plane splits" (similar in purpose to the FP-splits performed with GHRS on HST). In the classic sense, FP-splits are performed by taking spectra at several different focal plane assembly X-positions in the MDRS (or in principle, HIRS) apertures, thereby shifting the spectra in the dispersion direction on the detector. If the S/N is high enough in the individual spectra, they may be used to derive the source spectrum and the unshifting fixed pattern, which can then be removed from the data. With lower S/N data, aligning and averaging the spectra will help to reduce the fixed-pattern noise.

Operational implementation of classic FP-splits for FUSE is complicated by the difficulties in maintaining accurate coalignment of the different channels. For LWRS observations, the time-varying channel misalignments will cause the offsets of the spectra to differ somewhat from the planned steps of the FP-split sequence. For MDRS observations, the data lost to time-varying channel misalignments may complicate the FP-split analysis. Please see the discussion of channel coalignment in section 1.2.1.

A study of several observations employing the FP-SPLIT procedure has shown that data quality close to that expected from photon noise can be achieved using standard MDRS four-position FP-SPLITS. In these observations S/N ratios up to about 100 have been achieved. For most segments, the integration time required is between 0.5-1.0 times that based purely on photon statistics, **per FP-SPLIT position**. The exact number depends on the wavelength and detector segment used. In other words, a proposer should normally request four times the exposure time needed to get the desired photon noise. A more extensive report on the FP-SPLIT study can be found at the FUSE data analysis site under [FP-SPLIT white paper](#)

Refer to the [Phase 2 Instructions](#) for more information about the FPSPLIT special requirement. The XOFF special requirement is of less utility than FPSPLIT and will no longer be supported.

3.2.5 FES Images

The primary function of the FES CCD camera is to acquire target fields and provide fine pointing data to the spacecraft Attitude Control System. Additionally, the FES can provide visible pictures of the target field, for possible later use by the observer. At the discretion of Mission Planning, a so-called "FES science image" of the target field will be obtained during every spacecraft observation, usually at the end of the last exposure. (Note: a spacecraft observation potentially can be made up of many exposures scattered over multiple orbits.) The [Phase 2 Instructions](#) allow the investigator to specify the special requirement FESIMG and supply information about whether to take the FES image with the target IN or OUT of the observing aperture. FUSE Mission Planning will implement these requests on a best effort basis. Note that, as of Cycle 2, no requests for specific FES filters for these exposures are being accepted. When viewing FES images, users should be aware that the spectrograph apertures are NOT centrally located in the field of view, but are offset toward one side. Additionally, they will not be nicely aligned to cardinal points, but rather north and east will be rotated to a position driven by the spacecraft nominal roll angle at the time of the observation. The nominal target coordinates and aperture position angle will be provided with the processed image. Occasionally, for operational reasons, it becomes necessary to drop the default FES science exposure. In these cases, the user will still have access to acquisition (and reacquisition) images taken each orbit during the setup for an exposure. These FES images can be used for field verification, but will typically just show the target at some random position within a few arcmin of the spectrograph apertures. Hence, they do not provide information on the detailed pointing for an observation.

3.2.6 Unsupported Modes/Configurations

There are a number of possible modes or configurations that are not supported for normal operations. Any request for the use of such modes must be clearly documented and justified in the proposal and may or may not be implementable:

- Requests for multiple FES images. Use of the FES to monitor a target photometrically will not be supported. This can be done with ground-based telescopes, and is not a good use of FUSE resources. One confirmation picture of the target field will be obtained with the FES for each observation, as described above, plus images are obtained for each acquisition (or reacquisition) during an observation.
- Off-nominal roll angles. The roll angle of the FUSE satellite is managed to ensure that sufficient charge is generated by the solar arrays. This means that observations requesting specific position angles must be performed at specific times of the year. In the one reaction wheel attitude control mode, the spacecraft roll is also used to extent the periods of spacecraft stability. Please use the on-line [Position angle/Beta angle Calculator](#) to determine if and when roll-specific observations can nominally be performed. Note that attitude control considerations may override the nominal roll value.
- Off-nominal spacecraft beta angles. (Beta is the angle from the anti-sun position.) The satellite ACS seeks to keep FUSE pointed in a legal range of this angle from 15° to 115°, which defines the region of permitted target visibility. Operationally, it has been determined that **channel alignment can be managed much better within the 30 < beta < 85° range**, which is used for nominal operations. Observing outside this operational range (up the ACS limits) is possible in principle, but with greater attention spent on maintaining channel alignment and greater risk of failure. **As noted above in section 1.2.1., the current attitude control software is driven primarily by the need to manage torque and reaction wheel momentum, making considerations of off-nominal beta angles irrelevant in the near future. For cycle 8 no specific ROLL angle requests will be allowed.** The on-line [Position angle/Beta angle Calculator](#) will allow you to determine if and when your observations can nominally be scheduled.

Users need to be aware that requesting ANY extended capability may result in the requested observation remaining on hold for an indefinite period, and may prevent the scheduling of your targets! If you request any such capabilities, stay in contact with the project on developments so that adjustments can be made to your program if necessary.

3.3 Estimating Exposure Times

Assuming that Poisson noise dominates, the S/N ratio per resolution is given by

$$(S/N)^2 = \frac{S^2}{S + D + S_C} t$$

where S is the total number of events per second per resolution element from the source, D is the detector dark rate per resolution element, S_C is the scattered light event rate, and t is the integration time in seconds. This equation does not include the effects of fixed pattern noise, structure and/or uncertainties in the background subtraction, flux calibration, or wavelength calibration. All of these may degrade the S/N and limit the maximum achievable S/N ratio (e.g. [Section 2.5.1](#)). The height of a single resolution element is wavelength dependent because of the astigmatic nature of the spectrograph optics. Consequently, the dark level at any given wavelength can vary by as much as a factor of 2 from the average (see [Section 2.5.1](#)).

The FUSE team has developed a number of tools to help estimate exposure times. The FUSE Exposure Time Calculator, available on the [FUSE Planning Tools](#) page, is a web-based form which can calculate the observed signal to noise ratio given an exposure time or calculate the exposure time needed to achieve a given S/N ratio. Due to non-linear wavelength scales and differences between the channels, users requesting the highest performance may want to consider working with single channel data. This tool supports this calculation either for the total data set, or on a per channel basis. This information is requested from the user in the proposal. The ETC includes the most up-to-date information on instrument performance and effective area, and should be rigorous enough for almost any observing program. It can also provide reasonable estimates of total expected count rates from your targets (needed in Phase 2).

If your situation is not covered gracefully by the on-line tools, we refer you to [Appendix C](#) for a more detailed discussion of S/N calculation for FUSE spectra and some examples.

3.4 Scheduling

The planning and scheduling of FUSE observations begins with the proposal process, which consists of both a Phase 1 and (for successful proposals) a Phase 2 submission. Guest Investigators (GIs) submit Phase 1 proposals for one cycle of observing using a LaTeX template file and a formatted proposal. The primary goal of the Phase 1 step is scientific justification and proposal selection. The primary purpose of Phase 2 is to provide the FUSE planning system with verified coordinates and target information, and specify any scientific requirements that directly affect the scheduling of your observations.

The Phase 1 proposals and targets accepted by NASA are formatted into ASCII Phase 2 template files and returned to the appropriate GIs. GIs will be expected to modify (as needed) and verify the accuracy of the information in the Phase 2 template file, and resubmit it to the JHU planning system. In addition, specific information about instrument set-up parameters and scientific or scheduling constraints need to be communicated in the Phase 2 submission. An automated system has been set up to ingest Phase 2 proposals, check syntax and validity of keyword inputs, and populate the Mission Planning Database (MPDB). This database contains information on all targets currently under consideration for active scheduling. Note, however, that the Phase 2 text blocks describing feasibility and providing information about properly scheduling your program will be read and acted on by a *human being*; these text blocks are an active and important part of the Phase 2 inputs for FUSE. Refer to the separate [Phase 2 Instructions](#) for details of this process.

Mission Planning uses the target coordinates to obtain information on field stars surrounding each target location for use in field identification purposes. A small sub-set of the field stars will also be chosen to be FES guide stars. Other information needed by the planning system includes the satellite orbital elements, SAA models, torque authority and ground station contact times, which are provided by the Satellite Control Center. At this point, the MPDB will contain all of the necessary information for scheduling a given target and setting up the instrument properly. These data are used as input to a FUSE-specific version of the Spike scheduling tool used previously for scheduling aspects of the HST, EUVE, XTE, and ASCA missions.

Every observing program is assigned a unique identifying number (called the "program ID"). In addition, each target within the program is assigned a unique ID number, and each observation and exposure of that target is also numbered. The concatenation of these ID numbers provides a unique identifier for every exposure as it traverses the system from planning to on-board execution to data processing. The concatenated ID has the form PPPPTTTOOEEE (where P = program ID, T = target ID, OO = observation ID, and E = exposure ID). When the proposal database is first populated, only the proposal and target IDs are known. The exact number of exposures to be made is not known until the observation is scheduled, at which time the ID numbers assigned are written to the MPDB. The full ID of each exposure remains unique throughout the life of the mission.

A long-range plan (LRP) is generated based on the target pool, or some subset of the total targets, from the MPDB. This is done about once per week. The LRP is constructed in order to incorporate global planning requirements, allow tracking of time critical observations, and find the most efficient times to execute specific observations. In this mode, potential observations are placed in time "bins" (e.g., a particular week), but are not scheduled at the orbit-by-orbit level. The LRP provides a useful framework within which the more detailed short-term scheduling can be accomplished. Due to the scheduling restrictions imposed by the new attitude control system, the exact scheduling of FUSE observations is very complex and the order of observations important. In order to maximize the success rate of the observations, these motions must be managed. To implement this management and to allow the system to respond to real time events, the exact sequence of observations cannot be fixed at the LRP level. It is therefore important to note that while the LRP provides an invaluable tool to the FUSE mission planning, it is all the same a very dynamical document and does not provide a reliable source for the actual date of an observation.

A mission planning schedule (MPS) specifies a detailed (second-by-second) time-ordered sequence of activities and events to be carried out on-board during some period of time. An MPS typically covers a period of about one week although many deliveries have been one-two days long, particularly in cases of unforeseen spacecraft events. As the MPS is generated, targets are extracted from the current LRP bin and inserted into the MPS. Typically, it is not possible to include all the targets in the LRP bin into an MPS. The remaining ones are placed back in the pool and the LRP regenerated. The MPS is then delivered to the SCC, where the activity sequence is translated into detailed spacecraft and instrument command loads ("scripts") for uplink to the satellite.

3.5 Target Acquisition

The process of acquiring a target and placing it in the desired spectrograph aperture varies considerably in operational difficulty, depending largely on the aperture chosen (cf. section 2.3 above), the nature of the target, and the actual performance of the satellite itself. You need to know enough about the acquisition process to make intelligent decisions about the aperture to use and when your targets are likely to need an offset star for a good target acquisition. However, with the assignment of LWRS as the default aperture, much of the complication of target acquisitions has gone away. If you are observing in the LWRS aperture, little of this matters to you. But if you need the MDRS or HIRS apertures for your targets, you may need the information below. The [Phase 2 Instructions](#) provide detailed instructions on how to specify offset stars, in cases where they are needed.

We first discuss the general processes involved in target acquisitions and then discuss the different cases we encounter in real operations. The simplest case is that of a fixed (non-moving) point source. Acquisitions of extended objects, optically bright objects and moving targets present their own individual problems and are discussed below.

3.5.1 General Field Acquisition

An observation begins with a spacecraft slew to the object of interest. This will normally be done when the previous target becomes occulted by the earth. Assuming a relatively short slew length (20-40°), it will take only 5-10 minutes to slew between targets, which is less than the typical earth occultation period (30 - 40 minutes). The slew maneuver is calculated on the ground by the scheduling system and uplinked to the satellite to execute from stored command memory (i.e., observations are not conducted in real-time).

The accuracy of the slew (<5 arcmin [1 sigma] for slews up to 180°) are good enough to place the target within or near the FES field of view, which is roughly 19 arcmin square. When the target becomes unocculted by the earth, the IDS will send a previously stored command to the FES to take a short (~1 sec) exposure. In response, the FES will read out the CCD and send the digital image to the IDS.

After receiving the FES image, a process in the IDS will be invoked to locate the brightest stars in the image. These star locations will be used for field identification. Several bright stars will also be used for guiding while the IDS performs the field identification. The IDS determines the boresight pointing by comparing the star locations from the image with a table of star locations (from the HST Guide Star Catalog) produced by FUSE Mission Planners and uplinked for this purpose.

After sending the measured boresight pointing to the spacecraft ACS, the ACS will autonomously slew the satellite to correct the difference between the commanded and measured pointing positions. This will result in the target being placed in (or near, depending on the acquisition type) the desired spectrograph entrance aperture. The positions of selected guide stars are then centroided every second with the FES. Positions are sent to the IDS, which combines these positions (in a flux weighted manner) to produce a measured pointing. The IDS then sends this measured pointing value to the ACS, which in turn acts on this information to maintain pointing stability.

3.5.2 Types of Target Acquisitions

After the above operations are completed, and the satellite is guiding, then

1. The four channels will need to be aligned to maximize throughput (only if the HIRS aperture or MDRS has been selected), and/or
2. The target must be autonomously centered in all four spectrograph entrance apertures (which are located on the four FPAs). For the LWRS apertures, the target centering simplifies to centering the target in the aperture visible to the active FES. (Channels can be aligned approximately based on beta angle and alignment information on the previous target.)

The different target acquisition types are as follows:

1. FES Guide Star Acq
2. FUV PEAK-UP
3. FES Target Acq
4. FES Target Acq plus FUV PEAK-UP
5. Blind Offset from within FES FOV
6. Blind Offset from outside FES FOV

For more information, refer to [Appendix D](#) of this Guide.

3.5.3 Target Centering in the Aperture

After the small angle maneuver described above, the target will be placed within several arcseconds of the intended position. The method of centering your target depends on which aperture is being used and the properties of the target. For LWRS observations, the target is positioned well enough already, and the observation can proceed. For the most stringent cases, the channel alignment (if needed) and target centering both occur through the use of a single operational procedure known as an FUV PEAK-UP. To perform the PEAK-UP, the pointing of the satellite is dithered in a "step and dwell" pattern perpendicular to the aperture (in the X direction) to find the maximum FUV signal from the target (through each aperture if channel alignment is needed). The dwell time required at each step in the process depends on the expected FUV flux from the target, but we have had good results using a standard 10 second dwell time per step (across the board). If all four channels are aligned, then the signal will be maximized through each aperture at a common pointing. The data obtained in this peak-up process are used by the IDS to determine how much to move the FPAs and slew the satellite to center the target in all four channels. Once this step is completed, an FUV observation in MDRS or HIRS can begin. PKUPs are not performed in the LWRS apertures because the range of motion required is too large to be accomplished with FPA motions alone.

Since the vast majority of observations will use the LWRS apertures, further details regarding PEAK-UP acquisitions has been deleted from this document. If you need further information about this technique, refer to [Appendix D](#) of this Guide or contact the FUSE team via the [fuse support](#) e-mail account.

3.5.4 Optically Very Bright Targets

Targets that are very bright in the optical, but faint in the FUV (such as late type stars), present a special operational challenge. These targets will be very saturated even in a short FES exposure, and may also have large amounts of scattered light, possibly making it difficult to perform field acquisition or PEAK-UP. Tests of the have been promising; it appears that scattered light from a bright star may only be a serious problem for stars or planets with $V < 1.5$ (e.g., Arcturus or Jupiter). For such targets, we will perform the field acquisition step on a nearby offset field which does not include the bright target, and blind offset the target into the LWRS aperture. The accuracy of this step will depend on the accuracy of the target coordinates in the guide star frame of reference. It is not clear whether such targets will be observable in the MDRS or HIRS apertures.

For targets in the range $V = 1.5$ to 9, the target itself will be saturated in the FES, but we expect to be able to acquire guide stars in most cases. Hence, FES Guide Star Acq will be planned with these sources unless inspection of the available guide stars indicates a problem.

3.5.5 Extended Targets

The FUV PEAK-UP process will not work for extended sources (such as supernova remnants or elliptical galaxies), and must be performed on a nearby FUV bright offset target if channel alignment is needed. Then one of two things can be done to acquire the target (depending on the accuracy of the aperture positioning required). Usually an FES Guide Star Acq of the field surrounding the target position will be sufficient, especially if the "target" position has been provided in the reference frame of the guide stars themselves. (Positioning in this case should be to better than about 2 arcsec.) Optionally, if higher precision is required the slew could be commanded to an optically bright ($V < 13$) star very close to the extended target, and whose relative location with respect to the target is well determined. The position of this star can be centroided with the FES, but then a final offset is commanded to put the extended science target in the desired aperture.

3.5.6 Targets in Crowded Fields

Crowded fields can cause acquisition problems in one of several ways. For instance, stars with visual magnitudes comparable to your target and within about 20 arcsec in position may adversely affect the ability to perform the FES Target Acq scenario. Alternatively if the target is an FUV-bright target in an "optically" crowded field, then the real issue could be one of guide star availability. For example, take the case of a UV bright star in the center of a globular cluster. It may be very difficult to find isolated stars that can be used for guiding. Situations like this must be assessed on a case-by-case basis.

Another kind of crowded field is one containing several close-by FUV bright stars. In this case, guiding is not an issue, but target acquisition (or target isolation) is. For example, star fields in the Large Magellanic Cloud have proven problematic at times, especially using the default LWRS (30 arcsec) apertures. If only a single contaminating star is nearby, the MDRS aperture could be used at a specific position angle to avoid the nearby star (although this constrains when the observation can be scheduled). Investigators should alert FUSE Mission Planners of possible crowded field complications in their Phase 2 submissions.

3.5.7 Moving Targets

Proposals for Moving Targets will not be considered for cycle 8.

The ability of FUSE to acquire and track Moving Targets (MTs) has been tested and demonstrated during observations of several Solar System objects. FUSE has to date successfully observed Saturn's satellite Titan, the Io plasma torus, the northern and southern auroral zones of Jupiter, Mars, and several Comets. One of the comets was moving at an apparent rate of ~ 0.05 arcsec/sec.

In principle, FUSE can observe any MT whose apparent motion is up to 0.2 arcsec/sec. The spacecraft follows a trajectory defined in an uplinked table of positions as seen from FUSE (i.e., a parallax-corrected ephemeris). The pointing is updated once per second through a linear interpolation of coordinates in the table. Tracking is normally performed on Guide Stars (GSs) within the field of view of the FES. The jitter about the commanded motion in this case should be less than a few tenths of an arcsec, the same as for fixed targets.

For some MTs (e.g., comets, faint satellites), the target position can be refined by determining the centroid of its image in the FES. Then an ephemeris correction can be calculated onboard the spacecraft, and the target can be placed accurately in the selected aperture. While the target is in the aperture, accurate tracking is maintained by keeping stars in the FES moving in the direction and at the rate predicted by the target's ephemeris.

For MTs that are too bright to be acquired directly in the FES (e.g., planets, bright satellites), an acquisition is performed at a nearby field and an offset slew is executed to acquire the GSs in the MT field. Any ephemeris offset between the GSs and the target (e.g., due to the inaccuracy of either the Guide Star Catalog or of the target ephemeris itself) in this case will not be removed, and the absolute pointing will be determined by the absolute accuracy of the Guide Star Catalog (i.e., approximately 1 to 3 arcsec, depending on location in the sky) and the target's predicted ephemeris. If an accuracy of better than ~ 3 arcsec is not needed for a particular observation, then this mode may also be used for targets that could be acquired directly in the FES because it is simpler to implement.

FUSE also supports a "satellite tracking" mode, in which an MT at a known, fixed distance from the scientific target can be used for guiding, while the target itself is in the aperture. For example, one might use this mode to observe a planet while tracking on one of its satellites, if the relative position of the planet and satellite do not vary significantly during the

course of the exposure. However, GS tracking is generally preferred during MT observations, if suitable GSs are available.

During phase 2, FUSE MT observers will be asked for various details about their targets and observations in order to facilitate the accurate calculation of ephemerides and to enable accurate target acquisition and tracking. The target information that is needed is similar to the information that is provided by planetary observers who observe MTs with the Hubble Space Telescope (HST). For FUSE observations of comets and asteroids, heliocentric orbital elements must be provided. For planets and their satellites, the target's name is usually sufficient. If the target is a non-standard location (e.g., a specific latitude and longitude on a planet or satellite, or an offset from the nucleus of a comet), then that information must be provided as well. The FUSE Mission Planning team will use the target information provided by the observer to calculate the target's ephemeris using MOSS, which is the software system used and supported by the STScI for planetary observations made with the HST. Some new capabilities have been added to MOSS specifically to support the planning of FUSE MT observations. This system has been used to support all of the FUSE MT observations made to date and appears to work very well.

Some restrictions that apply to FUSE MT observations are outlined in [Section 3.6.5](#).

3.6 Restrictions

3.6.1 Short Observations and Minimum Observing Time

Observers will be charged a minimum of 4000 seconds for any observation regardless of the requested integration time <4000 seconds, except for SAFTSNP observations for which 2000 seconds will be charged. The actual on-source integration may be filled out to complete an orbit depending on the observation schedule and provided that the longer observation would not exceed a S/N ratio greater than 30:1 at full resolution (see [Section 3.6.3](#) below). This restriction especially applies to SAFTSNP observations, which in practice may have very short exposure times (see Section 3.1.3). This is done partially to account for the large overhead such observations cause in operations.

3.6.2 "Over-Bright" Targets

Proposal for over-bright targets will not be considered for cycle 8. Note, though that the bright limit for SiC ONLY or LiF2-HIRS ONLY observations for Cycle 8 has been set to 5.0×10^{-10} ergs cm⁻² s⁻¹ Å⁻¹

Given the sensitivity of the FUSE instrument, targets that are bright in the far ultraviolet present a particular challenge to the mission operations team. Sufficiently high local count rates may damage the microchannel plates, and there is a limited amount of charge that can be extracted from the microchannel plates during their lifetime. There are also limitations in the detector count rates (see sec. 2.5) which can corrupt the data and, at very high count rates (~46,000 c/s in one segment), cause autonomous detector shut downs. These hard limits are set in counts space, but correspond to less than an order of magnitude above the nominal bright limit.

The nominal bright limit of the FUSE instrument is 1.0×10^{-10} ergs cm⁻² s⁻¹ Å⁻¹ at any wavelength in the 900-1200 Å band, except for SiC ONLY and LiF2-HIRS ONLY observations for which the bright limit is 5.0×10^{-10} ergs cm⁻² s⁻¹ Å⁻¹. This applies also to emission line objects. In particular, emission line objects are limited to a maximum flux of 3.3×10^{-12} ergs cm⁻² s⁻¹ per 0.033 Å (10 km s⁻¹) resolution element at any wavelength in the FUSE bandpass. The limiting flux scales with the width of the line (e.g., a line with a width of 20 km s⁻¹ can have a maximum integrated line flux of no more than 6.6×10^{-12} ergs cm⁻² s⁻¹). Hence, expected line width information is an important part of estimating emission-line object feasibility and safety. Given that intrinsic line widths are not always known, as extra measure of conservatism is in order for emission line sources, especially if fluxes are variable or uncertain.

While the nominal FUSE bright limit is still in effect, there are specialized observing procedures by which targets with brighter targets may be observed. Such observations require additional instrument and planning resources and therefore constitute a limited resource. Only programs for which suitable targets below the FUSE bright limit cannot be identified should propose to use these techniques.

While users are encouraged to justify and suggest which specific techniques should be used for any given proposed observation, the final implementation of each accepted observation will be decided by the FUSE Science Operations team, in consultation with the Project Scientist and mission PI.

Techniques for observing "over-bright" targets include:

- **HIRS observations.** With the somewhat lower throughput of the HIRS aperture, targets with fluxes marginally above the FUSE bright limit ($<1.5 \times 10^{-10}$ ergs cm⁻² s⁻¹ Å⁻¹) may be observable through the HIRS aperture. Because of thermal channel motions, only target placement in the LiF1 (guiding) channel can be controlled accurately. For LiF2 ONLY observations through HIRS the limit is $<5.0 \times 10^{-10}$ ergs cm⁻² s⁻¹ Å⁻¹.
- **SiC-only observations.** With the lower effective area of the SiC channels (for a given wavelength) the extracted count rate is less when observed using the SiC optics than for the LiF optics. Hence, for somewhat over-bright objects (about within a factor 5), where the important science is restricted to wavelengths shortward of ~1100 Å, observations can be performed in SiC-only mode.
- **Observation with a de-focused telescope** By significantly defocusing one of the telescopes a spot much larger than the width of the HIRS aperture can be generated at that FPA. The flux seen by the detector is then determined by the fraction of the spot that is transmitted through the slit. Using this technique targets significantly above the FUSE brightness limit (factor 8-20) may be observed. However, this technique does **not** provide any photometric information. Also, shadowing effects from the grid wires (c.f. sec 2.5.4) are likely to occur with varying degrees of severity. Correcting for the increased grid wire shadows will probably require an FP-split procedure. Defocusing will only be done for one side of the instrument (with the other side inactive).
- **Low High-Voltage Observations** By lowering the detector High-Voltage (HV) well below the nominal setting, the count rates can be similarly lowered into an acceptable range. Studies are under way to ascertain whether source spectra can reliably be recovered using this technique. It is likely that FP-SPLIT techniques will be required to eliminate small scale artifacts when using this observing technique.
- **Scattered Light Observations** The large angle instrumental scattered-light profile has recently been investigated by the FUSE project. At 10" offset, an attenuated flux of $F_{\text{obs}}/F_{*} = 3.5 \times 10^{-4}$ is found while at 20" offset the attenuated flux is $F_{\text{obs}}/F_{*} = 1.0 \times 10^{-4}$. For very bright targets, this scattered light can be used to observe the target. Because of the thermal drifts, offsets less than 10" will, likely not be considered for any channel except LiF1. Note also, that the steepness of the scattered light profile together with thermal drifts introduce significant flux uncertainties in channels other than LiF 1.

In order to safeguard the instrument these techniques are normally combined with high-voltage management of the detector segments, such that only the minimally required number of detector segments are at full voltage for each observation.

Of the above techniques, only the first two have, to date, been successfully used for science observations. As all of these techniques are non-standard, users who wish to propose targets above the FUSE bright limit are strongly encouraged to contact the FUSE project at JHU for further consultations prior to submitting such proposals.

Observers will be required to demonstrate that their proposed targets do not exceed the bright limit, or to justify the use of the techniques discussed above. Flux levels can be estimated using previous observations in the 900-1200 Å band or fluxes extrapolated from a UV observation below 1800 Å using a model stellar atmosphere (for instance) or other model predictions. If the source has not previously been observed in the vacuum UV, if the source has a poorly determined FUV flux, or if the source has a flux greater than 5.0×10^{-11} ergs cm⁻² s⁻¹ Å⁻¹, the mission operations team may require an initial snapshot (SAFTSNP) observation to verify the source flux. *Any SAFTSNP exposures will be charged against the allocated observing time for that program, and guest investigators should budget 2000 seconds for this time in their Phase 2 proposal information.*

3.6.3 Night Only Observations

Observations of faint objects, particularly in the LWRS aperture, may be adversely affected by terrestrial airglow and the uncertainties in the scattered light distribution, as well as the uncertainties in the detector background (see section 2.5.1, above). Airglow and scattered light effects may be significantly alleviated by analyzing only the night-time portion of an obtained data set. Because FUSE cannot easily be retargeted within orbits, the scheduling of night-only observing is extremely inefficient and there is therefore no "night-only" mode of observing with FUSE. The way a required amount of night time data is to be requested is to multiply the desired time by a factor 1.6 which corresponds to the average ratio of total exposure time to night exposure time. The night-time data can then be extracted using the CALFUSE pipeline to screen out unwanted time intervals.

3.6.4 Signal to Noise Ratio Limits

Fixed-pattern noise in the detectors limits the routinely achievable S/N ratios to about 25-30:1. Higher S/N observations are achievable, using FP-split procedures (see section 3.2.4). *Guest investigators requesting observations with S/N ratios greater than 30:1 should strongly justify the need for high S/N in their proposal.*

3.6.5 Moving Target Restrictions

Although FUSE has a demonstrated capability to observe moving targets (MTs), proposers should be aware that the planning of MT observations generally requires significantly more time and effort than that needed for inertially fixed targets. For this reason, proposers are asked to keep their MT programs as simple as possible, consistent with the scientific objectives of the investigation. The more demands on mission capabilities and resources that are made by a program, the more stringent the requirements will be on its scientific justification, as provided in the proposal.

As is the case for fixed targets, MT observations will normally be scheduled for execution when the beta angle is between 30° and 85°. However, observations outside of this range may be considered when scientifically justified, subject to the constraint that the beta angle must not exceed 105° under any circumstances. Proposers should be aware that observations performed outside of the nominal beta angle range (30-85°) will likely suffer from significant channel misalignments, and the target may drift out of the aperture for all channels except for the one used to control the tracking (LiF1).

MT programs must also satisfy the same RAM constraints as other programs (i.e., no observing within 10° of the FUSE orbital plane). The latter restriction is particularly important for objects near the ecliptic plane, as those targets often violate the RAM constraint for a significant fraction of the time that they satisfy the beta angle constraint. Proposers can use the [FUSE CVZ/RAM tool](#) to assess the effect of the RAM constraint on their programs. This tool requires (RA,DEC) input for the target, which means supplying time-dependent values for MTs. Especially if you require observations of an MT at a particular time, you should check that both the beta angle and RAM constraints are satisfied.

3.6.6 Slit Position Angle Constraints

Specific ROLL (Slit position-angle) requirements will not be considered in cycle 8.

Because of spacecraft roll constraints, the aperture position angle on the sky will be a function of target position on the sky and time of year. Therefore, observations that require a specific aperture position angle will can only be performed at certain times when spacecraft constraints allow. Use the on-line "[Slit Position Angle Calculator](#)" on the FUSE Planning Tools web page to verify requested orientations occur at allowed times. Allowed times must take into account the pre-designated range of beta angle (Beta=30 to 85 degrees nominal) over which the FUSE spacecraft is operated, where beta is the angle between the anti-solar direction and the line-of-sight. Note that slit position angle requests are effectively time-constrained observations, and hence difficult to schedule. Please provide as much flexibility as possible when requesting this resource.

3.6.7 Beta Angle Constraints

Onboard power generation, via the solar arrays, requires that the angle between the spacecraft bore sight and the anti-Sun direction (beta angle) nominally stays within the range of 15<beta<105°. However, soon after launch it was discovered that the relative alignment of FUSE's four optical channels changes slightly, but systematically, as we point around the sky. To first order, these motions depend on the beta angle and are believed to result from the changing thermal environment caused by varying spacecraft attitude. They are repeatable at the ~5 arcsec level within some modest range of beta angle from about 30 to 85°. Further, but secondary, parameters have also been identified, including a diurnal variation as well as whether the target is in the Continuous Viewing Zone or not. At lower and higher beta angles these motions are less well-behaved, and we have tended NOT to plan targets in these ranges except for certain special cases. Consequently users should note that special considerations must be used to observe targets at beta angle below 30° or higher than 85°, especially if SiC channel data (shortest wavelengths) are required.

When staying in the 30 - 85° beta zone, we have had good success in observing successive targets in all four spectrograph channels when using the LWRS (30 arcsec square) apertures. In reality, we sequentially schedule targets in subsets of this range so as to minimize the amount of required channel alignment management and maximize the success rate. In the limit of unconstrained planning (e.g., lots of targets to choose from and no special timing or observational constraints), FUSE-Mission Planning can schedule a sequence of observations that minimize beta angle and slew motions between targets and maximize our chances of keeping the channels aligned. For targets with constraints such that larger changes of beta angle are required, some channel misalignment cannot always be avoided. Since the guiding is slaved to the LiF channels via the Fine Error Sensor camera (in normal operations to LiF1), the signature of such misalignment tends to be loss of signal in the SiC (short wavelength) channels.

There are also channel motion on orbital time scales. These are large enough to move targets in and out of the 4 arcsec aperture of the MDRS slit (and, of course, the 1.25 arcsec HIRS slit) in a fraction of an orbit. For targets with sufficient flux, it is possible to observe in all 4 channels using the MDRS aperture by performing multiple peakups during an orbit. However, observing in this mode is very inefficient (typically 30%-50% less exposure time per orbit than for LWRS observations), and the SiC channels will be misaligned 30%-40% of the time despite the additional peak-ups, further reducing observing efficiency.

Because of these effects, LWRS is considered the default observing aperture unless other constraints, say concern about airglow contamination, are important to the science. For observations only requiring LiF channels, there is no problem observing with MDRS, but if short wavelength data (<1010 Å) are needed, use of MDRS is discouraged.

3.6.8 Ram Angle Avoidance Constraints

Due to the detrimental impact of gases in the Earth's upper atmosphere on the optics of previous space astronomy missions, FUSE has, up until June 2005, implemented a zone of avoidance around the orbital plane of the spacecraft, referred to as the RAM zone. With the decrease in Solar activity as the Solar cycle minimum approached, the Earth's atmosphere has now shrunk enough that the RAM avoidance constraint can be removed.

Since slewing across the ram zone is a safety issue, as well as for thermal stability reasons, we try to minimize the number of equator crossings. This means that we typically schedule in the "north" (in actuality, "above" the ram zone) for 2-3 weeks, and then observe in the "south" for 2-3 weeks, etc. For targets with very long series of monitoring observations or with strict requirements on the spacing of observations this can also influence the schedulability. The issue of hemisphere crossings is even more acute under the newest attitude control system. At this time of writing, this is still a poorly understood aspect.

3.6.9 Magnetic Torque Authority

The nominal attitude control system on FUSE relied on reaction wheels aligned with the three primary spacecraft axes, and a fourth skewed wheel with components of angular momentum along each axis. In response to the failure of two of these reaction wheels in late 2001, the attitude control system was reconfigured to use the remaining two reaction wheels and the onboard Magnetic Torquer Bars (MTB) to achieve full control of the spacecraft. (The MTBs are basically dipole electromagnets whose original purpose was to allow momentum off-loading (spinning down) of the reaction wheels). The torque produced by the MTBs depend on the instantaneous strength and orientation of the Earth's magnetic field, at the location of the spacecraft, and the orientation of the spacecraft. Therefore, the possible torque produced is a complicated function of time and spacecraft orientation. The maximum magnetic field available from the MTBs is not strong enough to control the differential gravitational disturbances for all combinations of time and observational parameters. At any given time, only a restricted part of the sky can be observed while maintaining full attitude control.

Following the loss of the third reaction wheel in December 2004, a further modification of the attitude control scheme was implemented, relying on the remaining reaction wheel and the three MTBs. In this scheme, the management of reaction wheel momentum is a major concern which is likely to drive the scheduling of the spacecraft operations.

3.7 Time Critical and Monitoring Observations

The FUSE Operations team can handle a limited number of requests for time critical or monitoring observations, consistent with the available special resources required to implement such observations, and the capability to slew the satellite to the required beta angle. The most stringent of these is "Target of Opportunity" (ToO) observations, where rapid response to some temporally unpredictable event is required. In the primary mission the requirement was for the FUSE Operations team to respond to such a phenomenon within 48 hours. In the extended mission we estimate response times between 2 and 5 days, depending on when such a ToO is activated. Because of the disruption to ongoing operations and other stresses on the ground system, the availability of this resource will be limited. ToO's not requiring such rapid turnaround are less difficult. However, as with ANY time-specific observation, *the FUSE project cannot guarantee channel alignments without careful preparations and management of changes in beta angle.* This may affect our ability to perform ToO observations.

We also a limited number of "ephemeris" observations, or observations of periodic phenomena at a requested phase of the periodic cycle. These require special attention by both FUSE mission planners and the observer, and hence are considered "constrained". Such observations will need to be placed in the schedule at the appropriate time and "locked down", which involves special work on the part of planning personnel and also restricts observation planning directly prior to and after the scheduled observation, removing flexibility from scheduling. Beta angle (channel alignment) issues also come into play. The need for this capability should be mentioned in Phase 1, but details are not needed until the Phase 2 inputs are requested. The NRA for each cycle of FUSE proposals states the expected level of support for such observations.

The simplest kind of "time critical" observation for FUSE to handle is a monitoring observation, where a source is observed periodically at some nominal time separation, within some specified tolerance. Such observations can be scheduled with information provided in Phase 2, but they can be restrictive in terms of the scheduling of other observations (especially in terms of channel alignment), and should not be requested frivolously. More complicated monitoring programs, with uneven time sampling, can be handled in principle, but may require hand scheduling. It may be impractical to monitor bright sources on short timescales due to onboard memory limitations and limited downlink capability. Finally, any monitoring programs that extend beyond about a week to 10 days have the negative impact of pinning scheduling in one part of the sky for an extended period, where we may or may

not have sufficient other targets to fill in the schedule. (Again, this is largely driven by the need to minimize beta angle changes and manage channel alignment.) The need for and requirements on monitoring observations should be discussed in Phase 1 and specified explicitly in Phase 2 so that these impacts can be assessed.

4. Science Data Processing

4.1 The FUSE Pipeline Processing System

Once the data are transferred from the satellite to the ground, they are processed to produce fully reduced one dimensional spectra. In this section, we will briefly describe the FUSE data products and the calibration steps. Detailed descriptions of the CALFUSE pipeline and the output data products are beyond the scope of this document; the reader is referred to the [FUSE Data Handbook](#) for more information. A full FUSE dataset consists of the following files:

1. **Photon event files** (TTAG only)
2. **Spectral image files** (HIST only)
3. **Extracted spectra**
4. **Combined extracted spectra**
5. **Raw FES image files**
6. **Calibrated FES image files**
7. **Engineering snapshot files**

All FUSE data products are in FITS (Flexible Image Transport System) format with the data contained in binary extensions. Each exposure on a target produces independent SiC and LiF spectra for each detector segment for a total of 8 separate spectra (2 spectra (LiF+SiC) x 2 segments x 2 detectors). In TTAG mode, spectra for all three apertures are extracted, resulting in 24 1-D spectra (one aperture contains the target while the other two apertures contain airglow only). In HIST mode, only data for the target aperture are recorded on the satellite resulting in 8 1-D extracted spectra. In addition, the pipeline will generate 3 co-added spectra (one for each aperture) for TTAG exposures and 1 co-added spectrum for HIST exposures. Finally, the pipeline produces a merged spectrum for each observation (i.e. a co-addition of all the exposures). The co-added spectra are provided only for overview or quick look purposes and should not be used for scientific analysis. Depending on the source count rate, a single TTAG exposure generates 15-45 Mb of files. A typical HIST exposure generates about 10 Mb of files.

4.1.1 Processing FUV Spectral Data

The following steps are used by the FUSE calibration pipeline to transform the raw, two-dimensional data into a set of calibrated, one-dimensional spectra:

- **Data screening** (removes low quality or unreliable data);
- **Grating shift correction** (removes spectral motion due to grating rotation);
- **Drift correction** (calculates image stretch/shift due to thermal effects);
- **Background subtraction**
- **Flat-field correction**
- **Geometric distortion correction** (from electronic distortions in the the delay-line anode);
- **Astigmatism correction** (removes curvature perpendicular to the dispersion direction);
- **Doppler correction**
- **Spectral extraction**
- **Wavelength calibration**
- **Walk correction** (corrects for pulse-height dependent errors in the photon location).
- **Dead-time correction**
- **Flux calibration** (counts/second into $\text{erg cm}^{-2} \text{s}^{-1} \text{\AA}^{-1}$)
- **Channel co-addition** (for quick look analysis).

4.1.2 Processing FES CCD Images

The calibration steps to be applied to FES CCD images are more straightforward, and they follow typical CCD data reduction strategies:

- **bias level subtraction and trimming of the overscan regions**
- **dark subtraction**
- **flat fielding**
- **geometric rectification**
- **flux calibration**

The Fine Error Sensors will only be calibrated as well as necessary to ensure that they fulfill their target acquisition and guiding function. We will use exposures on standard star fields initially and monitor changes in routine observations of the white dwarf standards used for FUV calibration. In practice, this should result in magnitudes accurate to about 0.1 mag.

4.2 Data Distribution

All FUSE data is archived at the [Multimission Archive at the Space Telescope Science Institute](#) (MAST). Access is similar to that for archived HST data. Standard archive search techniques show summary information on observations, but only GIs and their designees will be able to view data in browse mode or submit requests to retrieve data sets during the proprietary period of six months. After the proprietary period, the FUSE data become publicly available. All requests for data will only be honored for registered archive users. See the [FUSE Archive](#) home page for details on how to register and how to access the archive. **When registering for a MAST account, you must specify that you want access to FUSE data.** See section 4 of the [FUSE Data Handbook](#) for more information.

4.3 Data Analysis Tools

Since the FUSE data products are in FITS format, they are compatible with most readily available astronomical software packages. These can be easily adapted by observers according to their tastes for viewing and analyzing the raw and calibrated data. Many readily available tools can be directly applied for measurement and analysis of the calibrated 1D spectra. The [FUSE Data Analysis page](#) has links to more detailed information and support software.

5. Further References

The FUSE project maintains a [web page of scientific overview and technical description papers](#) viewable on-line. Since this is updated regularly, we refer the reader there for further support.

Please send comments or questions to
fuse_support@pha.jhu.edu

[Return to the FUSE home page.](#)